Pharmacological Research 224 (2026) 108099

Contents lists available at ScienceDirect

Pharmacological Research

journal homepage: www.elsevier.com/locate/yphrs

A *Mangifera indica* L. extract functions as a broad TLR2/4/6 signalling rheostat to attenuate MyD88/NF-κB-driven inflammation and macrophage polarization☆

Anna Schettino [a], Anella Saviano [a], Noemi Marigliano [a], Martina Smimmo [b], Erika Esposito [b], Jenefa Begum [c], Areeba Fatima [c], Alyssa M. Urbanowski [d], Christopher Mahony [d,e], Amnah M. Khormi [f], Adel Abo Mansour [g], Tariq H. Iqbal [h], Helen M. McGettrick [d], Asif Jilani Iqbal [c,1,*], Francesco Maione [a,i,1,**]

[a] *ImmunoPharmaLab, Department of Pharmacy, School of Medicine and Surgery, University of Naples Federico II, Via Domenico Montesano 49, Naples 80131, Italy*
[b] *Department of Pharmacy, School of Medicine and Surgery, University of Naples Federico II, Via Domenico Montesano 49, Naples 80131, Italy*
[c] *Department of Cardiovascular Sciences, College of Medicine and Health, University of Birmingham, Birmingham B15 2TT, UK*
[d] *Department of Inflammation and Ageing, College of Medicine and Health, University of Birmingham, Birmingham, UK*
[e] *School of Infection and Immunity, Sir Graham Davies Building, Glasgow G12 8TA, UK*
[f] *Department of Hematology and Blood Bank, Jazan Specialist Hospital, Jazan, Saudi Arabia*
[g] *Department of Clinical Laboratory Sciences, College of Applied Medical Sciences, King Khalid University, Abha 62521, Saudi Arabia*
[h] *Department of Gastroenterology, Queen Elizabeth Hospital Birmingham NHS Foundation Trust, Birmingham, UK*
[i] *Nutraceuticals and Functional Foods Task Force, Department of Pharmacy, School of Medicine and Surgery, University of Naples Federico II, Via Domenico Montesano 49, Naples 80131, Italy*

ARTICLE INFO

Keywords:
Inflammatory bowel disease
innate immunity
macrophage polarization
Mangifera indica
monocyte transmigration
toll-like receptors (TLRs)

ABSTRACT

Current therapies for immune-mediated diseases often lack precision, causing broad immunosuppression. While *Mangifera indica* L. extract (here referred to as MIE) shows promise in resolving pain and modulating adaptive immunity, its direct impact on monocyte recruitment and macrophage polarization, remains elusive. Using a reverse translational approach, we examined the effects of MIE on primary human monocytes and macrophages from healthy donors and inflammatory bowel disease (IBD) patients. We assessed its ability to inhibit monocyte transmigration across TNF-α-activated endothelial monolayers and to modulate macrophage polarization along

Abbreviations: ADRB2, adrenoceptor beta 2; BSA, bovine serum albumin; *CCL17*, C-C motif chemokine ligand 17; *CCND1*, cyclin 1; *CD14*, cluster of differentiation 14; *CD40*, cluster of differentiation 40; COX-2, cyclooxygenase-2; DAMPs, damage-associated molecular patterns; DEGS, differentially expressed genes; DMSO, dimethyl sulfoxide; ECGS/H, endothelial cell growth supplement/heparin; EDTA, ethylenediaminetetraacetic acid; ELISA, enzyme-linked immunosorbent assay; FBS, foetal bovine serum; FLA-ST, flagellin from *Salmonella typhimurium*; HDBECs, human dermal blood endothelial cells; HMDMs, human monocyte-derived macrophages; IBDs, inflammatory bowel diseases; ICAM-1, intercellular adhesion molecule-1; IFN-γ, interferon-gamma; *IFI44L*, interferon-induced protein 44-like; IL, interleukin; *IL1R2*, interleukin 1 receptor type 2; *IL1RN*, interleukin 1 receptor N antagonist; I.p, intraperitoneally; IUPHAR, International Union of Basic and Clinical Pharmacology; *LIPG*, lipoprotein lipase G; LPS, lipopolysaccharides; LTA, lipoteichoic acid; MALP-2, macrophage-activating lipopeptide-2; M-CSF, macrophage colony-stimulating factor; MIE, *Mangifera indica* L. extract; MPGES-1, microsomal prostaglandin E synthase-1; MyD88, myeloid differentiation primary response 88; NSAIDs, glucocorticoid or nonsteroidal anti-inflammatory drugs; NF-κB, nuclear factor-kappa B; ODN, oligodeoxynucleotide; *NFXL1*, nuclear factor X-box binding like 1; *PARP11*, poly ADP-ribose polymerase 11; PBMCs, peripheral blood mononuclear cells; PBS, phosphate-buffered saline; PBL, peripheral blood lymphocytes; PEMs, peritoneal exudate macrophages; PGE_2, prostaglandin E_2; Poly I:C, polyinosinic-polycytidylic acid; PRRs, pattern recognition receptors; RT, room temperature; RNA-seq, RNA sequencing; *SOCS4*, suppressor of cytokine signalling 4; Th, T helper; Treg, regulatory T cell; TLRs, toll-like receptors; TNF-α, tumour necrosis factor-alpha; VCAM-1, vascular cell adhesion molecule-1; WT, wild type.

☆ This article is co-authored by a Consulting Editor. According to Journal's policy, the article has been handled by another editor independently, with the authors being blind to the whole process.

* Corresponding author.
** Correspondence to: ImmunoPharmaLab & Nutraceuticals and Functional Foods Task Force, Department of Pharmacy, School of Medicine and Surgery, University of Naples Federico II, Via Domenico Montesano 49, Naples 80131, Italy
E-mail addresses: a.j.iqbal@bham.ac.uk (A.J. Iqbal), francesco.maione@unina.it (F. Maione).
[1] These authors share senior authorship.

https://doi.org/10.1016/j.phrs.2026.108099
Received 18 November 2025; Received in revised form 12 January 2026; Accepted 13 January 2026
Available online 14 January 2026

Chemical compounds studied in this article:
Mangifera (CID: 23461)
Mangiferin (CID: 5281647)
DMSO (CID: 679)
IL-6 (CID: 3569)
TNF-α (CID: 91976359)

the M1/M2 phenotypes. Transcriptomic profiling via RNA-seq revealed several MIE-responsive pathways in human macrophages, which were subsequently validated functionally using murine peritoneal macrophages stimulated with a panel of distinct toll-like receptors (TLRs) agonists. MIE markedly impaired monocyte adhesion and transmigration across activated endothelium. In human macrophages, it selectively attenuated the pro-inflammatory M1 phenotype, robustly suppressing TNF-α secretion from both healthy donors and IBD patients, while exerting minimal effects on the M2 profile. Transcriptomic analysis revealed that MIE disrupts key inflammatory signalling networks, notably those governed by NF-κB and TLRs. Mechanistically, MIE did not exert broad TLR inhibition but instead acted as a precise immunological rheostat, dampening responses to murine TLR2, TLR4, and TLR6 agonists. TLR4-targeted modulation was mediated via downregulation of MyD88 and NF-κB expression, culminating in reduced pro-inflammatory cytokine production. We delineate a novel mechanism for MIE as a selective rheostat of the TLR2/4/6 axis for restoring innate immune homeostasis in inflammatory-based diseases.

1. Introduction

The innate immune system serves as the body's first line of defence, with macrophages acting as its key effector cells. Their critical role extends beyond pathogen phagocytosis to encompass remarkable functional plasticity, including the emerging concept of trained immunity [1], a *de facto* memory of innate immune cells driven by epigenetic and metabolic reprogramming, which leads to an enhanced response to secondary stimuli [2]. In response to microenvironmental cues, macrophages can polarize towards a classically activated (M1), pro-inflammatory phenotype [3], crucial for combating infections, or an alternatively activated (M2), anti-inflammatory phenotype [4], involved in inflammation, resolution and tissue repair [5]. A precise balance between these populations is essential for an effective immune response and the maintenance of homeostasis; conversely, an imbalance is a hallmark of numerous chronic inflammatory and autoimmune diseases [6], such as inflammatory bowel diseases (IBDs) [7]. The initiation of this process involves the recruitment of monocytes from circulation, orchestrated by a tightly regulated cascade of adhesion and transmigration across the vascular endothelium. This finely tuned mechanism becomes dysregulated in chronic inflammatory states, contributing to sustained immune cell infiltration and tissue damage [8]. Subsequent macrophage polarization is orchestrated by signals from pattern recognition receptors (PRRs), particularly toll-like receptors (TLRs) that

rapidly reshaping their transcriptional landscape in response to external stimuli [9,10], including nuclear factor-kappa B (NF-κB), driving the transcription of pro-inflammatory genes and promoting the M1 phenotype [11].

Our research group spearheads the comprehensive preclinical characterization of a proprietary *Mangifera indica* L. extract (MIE). This botanical, derived from the ubiquitous mango tree, possesses a rich ethnomedicinal history as a pleiotropic therapeutic agent, particularly within subtropical and tropical traditional medicine systems. Beyond its nutritional value, the mango (*Mangifera indica* L.) has been historically utilized for its broad-spectrum biological and immunopharmacological properties [12]. Our foundational work established its potent systemic anti-inflammatory and immunomodulatory activity, demonstrating its ability to dual target the prostaglandin E_2 (PGE_2) synthesis axis via inhibition of cyclooxygenase-2 (COX-2) and microsomal prostaglandin E synthase-1 (mPGES-1) [13], and to rebalance the adaptive immune response by modulating the pathogenic T helper (Th)17/ regulatory T cell (Treg) ratio [13]. We subsequently validated these findings using a robust reverse translational approach, confirming that MIE dampens the hyperactive inflammatory response in peripheral blood lymphocytes isolated from patients with IBD and is protective in murine models of colitis [14]. Most recently, we expanded its therapeutic profile by demonstrating that MIE targets the neuro-immune axis, effectively reducing visceral hypersensitivity and pain persistence, a major unmet clinical need in chronic IBD [15].

A critical mechanistic gap persisted in our understanding of MIE's full immunomodulatory potential: its direct impact on the earliest, decision-making events of the innate immune response. Specifically, we had not yet interrogated how MIE influences the initial recruitment of circulating monocytes, the precursors to tissue macrophages, or their subsequent fate determination through polarization and functional training. This gap is pivotal because the spatio-temporal control of monocyte recruitment and their phenotypic programming into macrophages are central, rate-limiting steps in both the initiation and resolution of inflammation. Addressing this question is essential to bridge MIE's known bioactivities with its potential to modulate the very genesis of an immune response [8,16].

To complete the mechanistic understanding of MIE's immunomodulatory action, this study investigated its influence on early events of the inflammatory cascade. We first demonstrated that MIE effectively inhibits the transmigration of monocytes through a layer of human endothelial cells. We then focused on its effects on human macrophage polarization. We examined MIE's effects on monocyte transmigration across human endothelial layers and on macrophage polarization using primary cells from both healthy donors and IBD patients. Functional assays, cytokine profiling, and transcriptomic analyses revealed that MIE attenuates pro-inflammatory responses in M1-polarized macrophages and modestly modulates M2 phenotypes. Bulk RNA sequencing (RNA-seq) data further implicated NF-κB and TLR signalling pathways, prompting targeted exploration in murine macrophages stimulated with a panel of TLR ligands. These data uncovered a selective inhibitory effect of MIE on TLR2, TLR4, and TLR6 mediated responses. Furthermore, we provide preliminary evidence that suggest that MIE may influence key mediators of trained immunity, pointing to a potential role in long-term immune regulation.

2. Materials and methods

2.1. Reagents and chemicals

Bovine serum albumin (BSA), dimethyl sulfoxide (DMSO), foetal bovine serum (FBS), phosphate-buffered saline (PBS), ethylenediaminetetraacetic acid (EDTA), glutaraldehyde, lipoteichoic acid from *Bacillus subtilis* (LTA), polyinosinic-polycytidylic acid [poly(I:C)], lipopolysaccharides (LPS) from *Escherichia coli*-O111:B4 and zymosan A from *Saccharomyces cerevisiae* were purchased from Sigma-Aldrich Co. (now under Merck, Darmstadt, Germany). Flagellin (FLA-ST) from *Salmonella typhimurium* and a Class A CpG oligonucleotide (ODN 1585) from InvivoGen (Rome, Italy). Imiquimod from Tocris Bioscience (Milan, Italy). Human CD14 microbeads were obtained from Miltenyi Biotech (Bergisch Gladbach, Germany). Medium 199 and RPMI1640 cell medium were obtained from Gibco™ by Thermo Fisher Scientific (Paisley, Scotland). Macrophage colony-stimulating factor (M-CSF) was from Peprotech (Cranbury, USA). For western blot analysis, NF-kB p65 was obtained from Cell Signaling (Danvers, USA), myeloid differentiation primary response 88 (MyD88) from Abcam (Eugene, USA), TLR4 from Abclonal Tecnology (Wuhan, China) and anti-β-actin from R&D Systems (Milan, Italy). HRP-conjugated IgG secondary antibodies were purchased from Bethyl Laboratories (Montgomery, USA). Unless otherwise stated, all the other reagents were from BioCell (Milan, Italy).

2.2. Source, characterization, and preparation of Mangifera indica L. extract (MIE)

The *Mangifera indica* L. extract (MIE), standardized to 90 % mangiferin (batch number: CMGD-C-A091434), was supplied and certified by L.C.M. Trading S.p.A. (Milan, Italy). The vendor's certificate of analysis is provided in Supplementary Figure S1. This specific batch has been fully chemically characterized by L.C.M. Trading S.p.A. (Supplementary Figure S2), and in our previous work [13] confirming its phytochemical profile. For all biological assays, the dry extract was solubilized in sterile DMSO to prepare a concentrated stock solution, taking into account the concentrations to be tested and the well volumes required for each experiment. The stock solution was freshly diluted in the appropriate culture medium immediately prior to each experiment. Based on the tested concentrations, the final DMSO percentages ranged from 0.033 % to 0.067 %. In all treated samples, the final concentration of DMSO never exceeded 0.1 % (v/v), which was considered the upper limit to ensure the absence of vehicle-related cytotoxicity *in vitro* cell-based assays. Appropriate solvent controls were included in all experimental setups.

2.3. Human ethics approval and research

This study was reviewed and approved by the University of Birmingham Local Ethical Review Committee (ERN_18–0382: Healthy Blood Donor Collection; 21/PR/0515: Exploration and validation of host and microbial biomarkers in newly diagnosed patients with immune-mediated inflammatory disease of the gastrointestinal tract [IMGID-INCEPTION]; IRAS: 287279; Protocol number: RG_21–009). Written informed consent was obtained from all participants prior to inclusion in the study. The study was conducted in accordance with recognized ethical standards, including the Declaration of Helsinki, the US Federal Policy for the Protection of Human Subjects, and the European Medicines Agency Guidelines for Good Clinical Practice. An equal proportion of male and female donors were included, with an age range between 20 and 40 years (Table 1) [14,17]. Human tissues used in this study were procured in line with the WHO Guiding Principles on Human Cell, Tissue and Organ Transplantation. Part of this research was carried out at the National Institute for Health and Care Research (NIHR) Birmingham Biomedical Research Centre (BRC). This research was supported by institutional and grant funding. The funders had no role in the design of the study, collection, analysis, and interpretation of data, or in the writing of the manuscript.

Table 1
Demographic, clinical and laboratory characteristics of IBD patients.

Age (years)[a]	37 (26–40)
Female; number (%)	1 (14.3)
Ethnicity White; number (%)	3 (42.9)
Symptom duration (months)[a]	3 (1–24)
Weight (kg)[a]	90.85 (72.20–108.7)
Height (m)[a]	1.77 (1.64–1.80)
BMI[a]	29.81 (25.04–33.55)
Smoker; number (%)	3 (42.9)
FCAL at baseline (μg/g)[b]	1577 ± (794.6)
CRP (mg/l)[a]	5 (1–24)
HBI[a]	9 (6–13)
Partial Mayo[a]	4 (3–6)
Endoscopic Mayo[a]	na
SES-CD[a]	6 (3–8)
Montreal Classification; Extent/Location (%)	E3: 2 (28.6)
Montreal Classification; Severity/Behaviour (%)	S2: 2 (28.6)
Treatment utilised (initiated after sampling)	-

IBD (N = 7)
Categorizing race and ethnicity= White and Asian. [a]median (interquartile range). [b]mean ±SD; BMI= Body Mass Index; CRP= C-reactive protein; FCAL= faecal calprotectin; HBI= Harvey-Bradshaw Index; na= not applicable; SES-CD= Simple Endoscopic Score for Crohn's disease; - = data not obtained from patients at time of presentation.

2.4. Isolation and differentiation of human monocyte-derived macrophages (hMDMs)

Blood was collected from adult healthy donors and patients with IBD. Patients were recruited from the gastroenterology Department of Queen Elizabeth Hospital and Birmingham Heartlands Hospital (Birmingham, UK) and their diagnosis was established by standard clinical, endoscopic, and histologic criteria [18]. All subjects were treatment-naïve, not receiving any form of medication (glucocorticoid or nonsteroidal anti-inflammatory drugs, NSAIDs) at the time the blood was taken (Table 1). Since patients are in the early stages of evaluation and diagnosis, the stage of disease or the status of remission has not been determined at the point of inclusion into this study. Peripheral blood mononuclear cells (PBMCs) were isolated from whole blood of healthy donors and IBD patients using histopaque® 1077 (Sigma-Aldrich) density gradients, as previously described [17,19]. Mixed monocytes were isolated from PBMCs, using PBS (without Ca^{2+} and Mg^{2+}) supplemented with 0.5 % BSA and 2 mM EDTA at 4 °C, by positive selection for CD14 using anti-CD14 microbeads (Cat. No. 130–050–201) and MACS LS separation columns both from Miltenyi Biotec (Bergisch Gladbach, Germany). Purified monocytes (~95 % purity; flow cytometry analysis is reported in Supplementary Figure S3) were cultured at 37 °C in 5 % CO_2 in RPMI 1640 medium (Gibco™ by Thermo Fisher Scientific; Cat. No. 11340892)/10 % FBS, containing 50 ng/ml M-CSF, which was replaced every two days for six days to achieve differentiation into naïve macrophages (Mφ; here referred as M0) [19,20].

2.5. Macrophage polarization and treatment

To induce "pro-inflammatory" (M1) or "pro-resolution" (M2) phenotypes, M0 macrophages were stimulated respectively with LPS (100 ng/ml; Sigma-Aldrich; Cat. No. L4524–5MG) and interferon-gamma (IFN-γ, 20 ng/ml; PeproTech, London, UK; Cat. No. 300–02), or with interleukin (IL)-4 (20 ng/ml; PeproTech; Cat. No. 200–04) for 24 h as previously described [17,21] and according to the experimental design shown in Fig. 1**A**. For experimental assessments, macrophages were co-treated (simultaneously, assessing direct interference) with either MIE vehicle (DMSO at the highest concentration used in test wells, 0.033 %) or MIE extract at the indicated concentrations [0.1–10 μg/ml for the assessment of tumour necrosis factor-alpha (TNF-α) and IL-10 levels; 1 μg/ml for RNA-seq analysis] for 24 h.

2.6. Static adhesion assay

Commercially sourced primary human dermal blood endothelial cells (HDBECs; PromoCell; Heidelberg, Germany) were cultured in endothelial cell growth medium MV (Promocell; Cat. No. C-22020). After 4 passages, HDBECs were seeded into 12-well tissue culture plates at a density yielding confluent monolayers. Prior to stimulation, HDBEC monolayers were washed with endothelial cell growth medium MV enriched with endothelial cell growth supplement, a bovine hypothalamic extract additional containing heparin (ECGS/H; PromoCell; Cat. No. C-30120), pre-warmed to 37 °C. Cells were then stimulated with TNF-α (100 U/ml; R&D Systems; Cat. No. 210-TA) for 4 h. Human monocytes from healthy donors were isolated as described above and were pre-treated (mimicking a preventive or priming effect on monocytes prior to endothelial interactions) with MIE extract (10 μg/ml) or its corresponding vehicle (DMSO, 0.033 %) in M199 media (Gibco™ by Thermo Fisher Scientific, Cat. No. 11150–059) supplemented with 0.15 % BSA for 30 min and subsequently added to the activated HDBECs for 7 min. Following incubation, wells were gently washed twice with warm M199 media to remove unbound cells and fixed with 2 % glutaraldehyde for 10 min at room temperature (RT). Glutaraldehyde was removed with several 1 ml washes of PBS (with Ca^{2+} and Mg^{2+}).

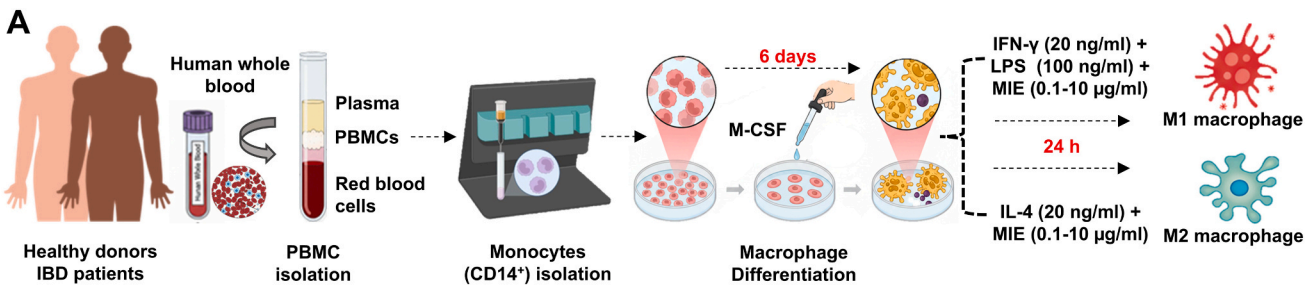

Healthy donors

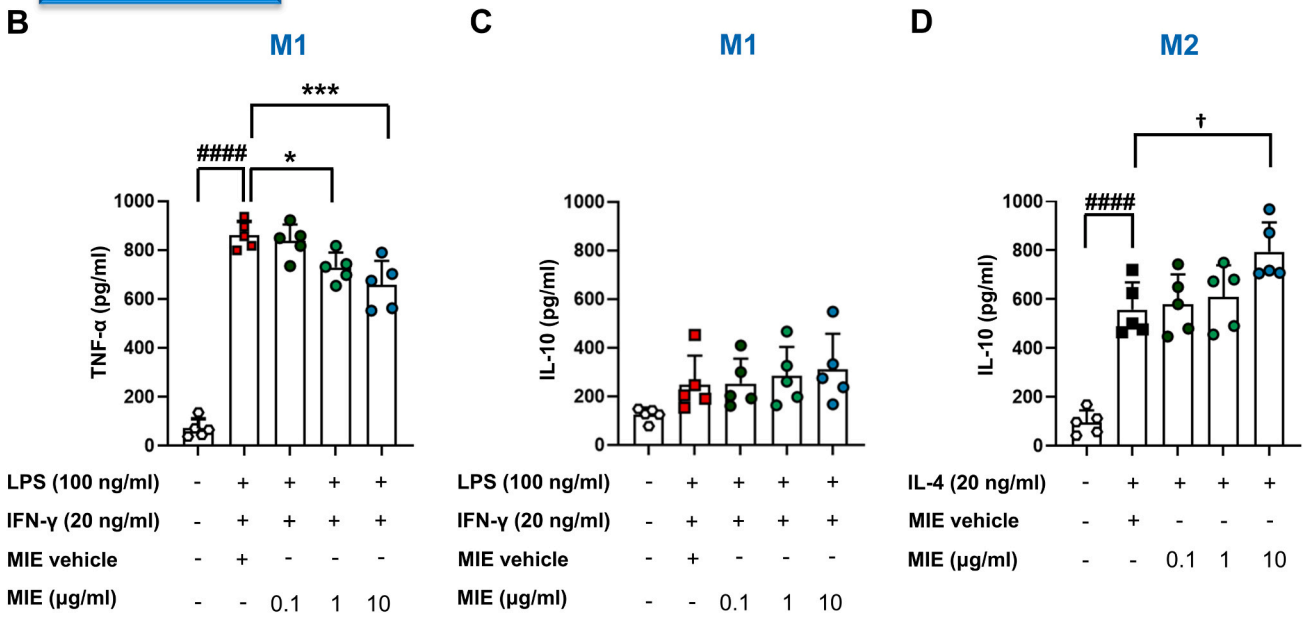

IBD patients

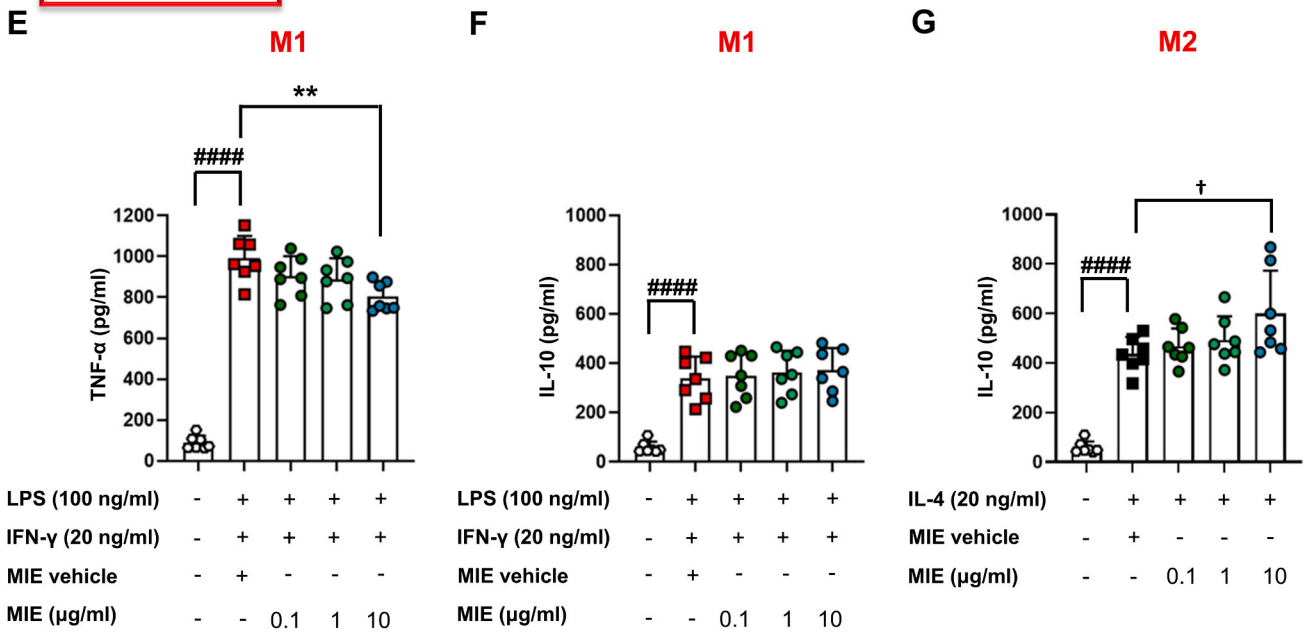

(caption on next page)

Fig. 1. Modulation of cytokine release by MIE in M1/M2 macrophages from healthy and IBD-derived monocytes. Schematic overview of the experimental design (**A**). Macrophages were derived from primary human $CD14^+$ monocytes isolated from healthy donors and IBD patients and differentiated with macrophage colony-stimulating factor (M-CSF) for 6 days (M0 phenotype). Resulting macrophages were then polarized towards M1 [LPS (100 ng/ml) and IFN-γ (20 ng/ml)] or M2 [IL-4 (20 ng/ml)] phenotypes and co-treated with MIE vehicle (DMSO at the highest concentration used in test wells, 0.033 %) or MIE extract (0.1–10 μg/ml) for 24 h (**A**). Supernatants were collected for the assessment of cytokine levels by ELISA assay (**B-G**). Specifically, TNF-α release was measured in M1 macrophages from healthy donors (**B**) and IBD patients (**E**), while IL-10 secretion was measured in both M1 and M2 macrophages for healthy donors (M1: **C**; M2: **D**) and IBD patients (M1: **F**; M2: **G**). Data are expressed as pg/ml and presented as means ± S.D. of N = 5 for healthy donors and N = 7 for IBD patients. Statistical analysis was conducted by one-way ANOVA followed by Bonferroni's for multiple comparisons. $^{\#\#\#\#}P \leq 0.0001$ *vs* M0 phenotype; $^{*}P \leq 0.05$, $^{**}P \leq 0.01$, $^{***}P \leq 0.001$ *vs* M1 + MIE vehicle; $^{\dagger}P \leq 0.05$ *vs* M2 + MIE vehicle.

Images were taken from five different fields in the centre of each well using phase-contrast microscopy (IX71; Tokyo, Japan). Images were analysed offline using Image-pro 7.0 software (Media Cybernetics, Rockville, USA), with adherent cells being defined as phase bright (rounded morphology), phase grey (activated/spreading morphology) or phase dark (transmigrated through the endothelium) (Fig. 2**D**). Monocyte adhesion was expressed as the total number of cells per mm^2, while transmigration was expressed as a percentage of total adherent cells [17].

2.7. RNA-seq

Human monocytes were isolated from healthy donors and differentiated into M0 macrophages for 6 days followed by subsequent polarisation into M1 and M2 phenotypes as described above and co-treated with either MIE vehicle or MIE extract (1 μg/ml) for 24 h. Total RNA was extracted using the RNeasy Mini kit from Qiagen (Hilden, Germany) according to manufacturer's instructions. RNA quantification and integrity was assessed using the Agilent 4200 Tapestation with High Sensitivity RNA ScreenTape from Aglilent Technologies (Santa Clara, USA) with all RIN scores exhibiting values greater than 7. Libraries for next generation sequencing were prepared using Quantseq 3'mRNA-seq Library Prep Kit FWD for illumina from Lexogen (Vienna, Austria). Bulk RNA-seq was performed at the Genomics Birmingham Facility (Institute of Cancer and Genomic sciences, University of Birmingham, UK) on an Illumina NextSeq 500/550 platform using a Mid output kit v2.5 (150 cycles) to generate 75 bp single end reads. Quality control of RNA-seq reads were performed using FastQC (v0.11.9) and adapter sequences were trimmed using BBMap (v39.19-GCC-12.3.0). Cleaned reads were aligned to the reference genome (GRCh38) using STAR (v2.7.11a-GC-12.2.0) followed by gene-level quantification obtained from feature counts using the Subread package. For differentially expressed genes (DEGs) analysis, lowly expressed genes were excluded, and batch correction was performed prior to downstream analysis using the DESeq2 package. Genes with an adjusted *P* value (FDR) ≤ 0.05 and a Log_2 Fold Change ≥ 0.42 were considered significantly differentially expressed for M0, M1 and M2 phenotypes in MIE *vs* MIE vehicle comparison. A total of 73, 75, and 172 genes met the significance and modulation criterion in M0, M1, and M2 macrophages, respectively [22,23].

2.8. Animals

Isolation of peritoneal macrophages was performed in accordance with UK legislation (Animal Scientific Procedures Act 1986) under the authority of the UK Home Office license PPL P50CB9C61: Leukocyte recruitment and retention in acute and chronic inflammation, with approval from the University of Birmingham Local Ethical Review Committee. All animal experiments were conducted in compliance with the ARRIVE (Animal Research: Reporting of *In Vivo* Experiments) guidelines. The study also adhered to the WMA Statement on Animal Use in Biomedical Research and the European Union Directive 2010/63/EU on the protection of animals used for scientific purposes, ensuring internationally recognized standards for experimental design, animal welfare, and pharmacological care.

Six to eight-week-old C57BL/6 J wild type (WT) mice (male) from Jackson Laboratories from Charles River, (Margate, UK) were housed with free access to food and water under SPF environmental conditions at 21 ± 2 °C, 55 ± 10 % relative humidity and a 12 h light-dark cycle. Conditions were qualified by screening using Federation of European Laboratory Animal Science Associations approved methods. All procedures were carried out to minimize the number of animals used and their suffering. Experimental study groups were randomized, and their assessments were carried out by researchers blinded to the treatment groups.

2.9. Isolation of murine peritoneal exudate macrophages (PEMs)

Peritoneal cells were harvested by lavage (PBS without Ca^{2+} and Mg^{2+}, supplemented with 3 mM EDTA) and collected in RPMI 1640 medium. Macrophages were then isolated from resident peritoneal exudate cells as previously described [24]. Briefly, cell suspension was plated in 6-well plates and incubated for 2 h in a humidified 5 % CO_2 at 37 °C. Following incubation, non-adherent cells were removed by performing three sequential washes with warm, serum-free RPMI 1640 medium. The resulting adherent cell population, representing the macrophage monolayer, was confirmed to be > 95 % pure based on morphological assessment [25], and was subsequently stimulated with various TLRs agonists, as described in detail below.

2.10. In vitro stimulation of murine peritoneal macrophages with TLRs agonists

Isolated peritoneal macrophages were treated according to two independent experimental schemes. In the first experimental setting (Fig. 5**A**), to assess the temporal dynamics of MIE's action, cells were exposed to MIE (10 μg/ml) in three pharmacological contexts relative to LPS (10 μg/ml) challenge: pre-treatment (30 min prior, mimicking prophylactic intervention), co-treatment (simultaneously, assessing direct interference), and post-treatment (30 min after, modelling therapeutic intervention post-inflammatory trigger) or its corresponding vehicle (DMSO, 0.067 %). In a second experimental setting (Fig. 6**A**), macrophages were pre-treated with MIE (10 μg/ml) for 30 min prior to stimulation with various TLR agonists, including LTA (TLR2 ligand; 3 μg/ml; Cat. No. L3265), poly(I:C) (TLR3 ligand; 25 μg/ml; Cat. No. P1530), LPS (TLR4 ligand; 10 μg/ml; Cat. No. L2630), FLA-ST (TLR5 ligand; 5 μg/ml; Cat. No. tlrl-stfla), Zymosan (TLR2/6 ligand; 10 μg/ml; Cat. No. Z4250), Imiquimod (TLR7 ligand; 2 μg/ml; Cat. No. 3700) and ODN 1585 (TLR9 ligand; 1.5 μM/ml; Cat. No. tlrl-1585) [26–29]. In both experimental settings, after 24 h of incubation, supernatants and adherent cells were harvested for subsequent *ex vivo* analysis [30,31].

2.11. ELISA assay

Enzyme-linked immunosorbent assays (ELISAs) for TNF-α (Cat. No. DY210) and IL-10 (Cat. No. DY217B) (both from R&D System) were carried out in supernatants from human M1 and M2 macrophages, derived from healthy donors and IBD patients. IL-6 (R&D System; Cat. No. DY406), TNF-α (Diaclone now part of Medics Biochemica, Espoo, Finland; Cat. No. 860.040.192) and PGE_2 (R&D System; Cat. No. KGE004B) levels in murine peritoneal macrophage supernatants were quantified by commercially available kits according to the procedure

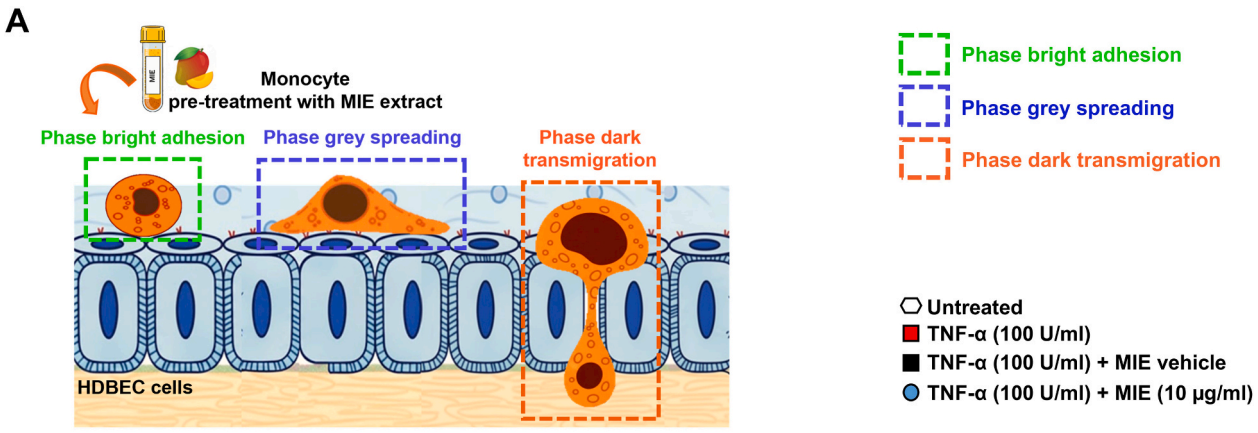

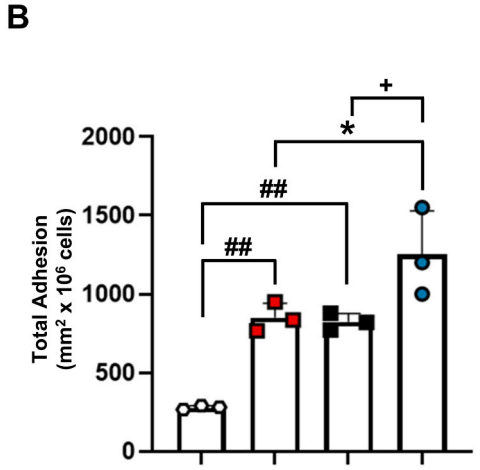

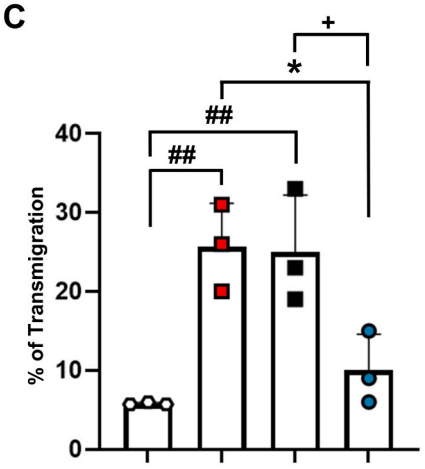

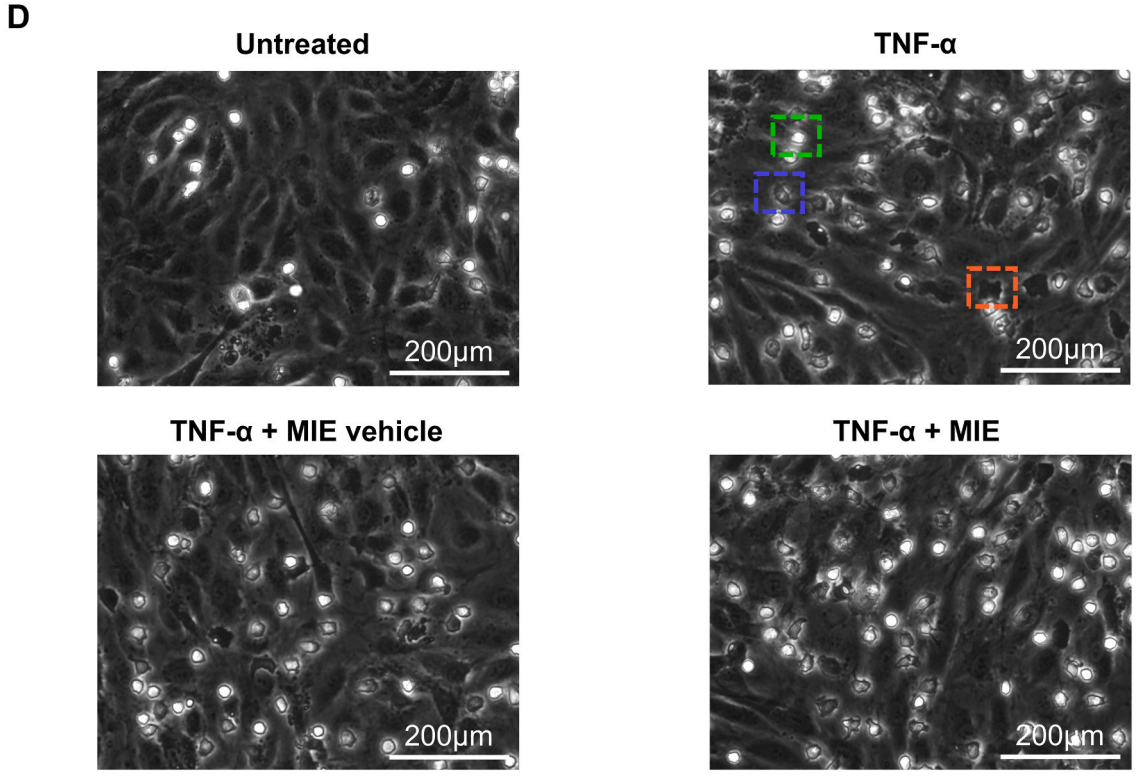

(caption on next page)

Fig. 2. Effect of MIE on monocyte adhesion and migration across human dermal blood endothelial cells (HDBECs). In a static adhesion/migration assay, HDBECs were stimulated with TNF-α (100 U/ml) for 4 h. Human monocytes from healthy donors were pre-treated with MIE extract (10 μg/ml) or its corresponding vehicle (DMSO, 0.033 %) for 30 min and then added to the activated HDBECs for 7 min. Non-adherent cells were subsequently removed by washing. In the panel **D** representative images (200 μm scale bar) of monocytes at distinct migratory stages (**A**) are shown: adhesion (indicated as phase bright and spherical in morphology, green square), spreading (indicated as phase grey and multipolar in morphology, blue square; quantified as % in Supplementary Fig. S4) and transmigration (indicated as phase dark and elongated in morphology, orange square). Quantification of monocytes total adhesion (expressed as mm^2 x 10^6 cells) (**B**) and % of transmigration (**C**) was performed using Image-Pro 7.0 software. Data are presented as means ±S.D. of N = 3 independent healthy donors. Statistical analysis was conducted by one-way ANOVA followed by Bonferroni's for multiple comparisons. $^{\#\#}P \leq 0.01$ *vs* Untreated; $^{*}P \leq 0.05$ *vs* TNF-α; $^{+}P \leq 0.05$ *vs* TNF-α + MIE vehicle.

described by Saviano *et al.* [32]. Briefly, 100 μl of supernatants, diluted standards, quality controls, and dilution buffer (blank) were applied on a pre-coated plate with the monoclonal antibody for 2 h. After washing, 100 μl of biotin-labelled antibody was added, and incubation continued for 1 h. The plate was washed, and 100 μl of the streptavidin-HRP conjugate or enzyme conjugate was added, and the plate was incubated for a further 30 min period in the dark. The addition of 100 μl of the substrate and stop solution represented the last steps before the reading of absorbance (measured at 450 nm) on a microplate reader (Multiskan™ GO Microplate Spectrophotometer; Thermo Scientific™, Waltham, USA). Antigen levels in the samples were determined using a standard curve, normalized to the sample volume, and expressed as pg/ml [14].

2.12. Western blot analysis

Peritoneal macrophages were lysed and subjected to SDS-PAGE (10 % gel) using standard protocols as previously described [14,33]. Briefly, proteins were transferred to nitrocellulose membrane (0.2 μm nitrocellulose membrane, Trans-Blot®TurboTM, Transfer Pack, Bio-Rad Laboratories, Hercules, CA, USA, RRID: SCR_008426) in transfer buffer (25-mM Tris–HCl pH 7.4 containing 192-mM glycine and 20 % v/v methanol) at 400 mA for 2 h. Membranes were incubated for 2 h with non-fat dry milk (5 % w/v) or BSA (4.5 % w/v) in PBS supplemented with 0.1 % (v/v) Tween 20 (PBS-T) at RT and then incubated at 4 °C with the appropriately diluted primary antibodies overnight: rabbit monoclonal NF-kB p65 (1:1000; clone D14E12; Cat. No. 8242S), goat polyclonal MyD88 (1:1000; Cat. No. Ab28763), rabbit polyclonal TLR4 (1:2000; Cat. No. A5258) and mouse monoclonal anti-β-actin (0.01 μg/ml; clone: 937215; Cat. No. MAB8929). After lavages with PBS-T, blots were incubated a 1:3000 dilution of related horseradish peroxidase-conjugated secondary antibody (Donkey anti-Mouse IgG Heavy and Light Chain Antibody HRP Conjugated, Cat. No. A90–137 P; Sheep anti-Rabbit IgG Heavy and Light Chain Antibody HRP Conjugated, Cat. No. A120–100 P or Donkey anti-Goat IgG Heavy and Light Chain Antibody HRP Conjugated, Cat. No. A50–101 P) for 2 h at RT and finally washed 3 times with PBS-T. Protein bands were detected by using the enhanced chemiluminescence method (Clarity™ Western ECL Substrate, Bio-Rad Laboratories,) and Image Quant 400 GE Healthcare software (Milan, Italy). Bands were quantified using the GS 800 imaging densitometer software (Bio-Rad, Milan, Italy) and normalized with respective β-actin [14,34,35]. Uncropped and triplicate original western blots are presented in **Original western blot file**.

2.13. Statistical analysis

Statistical analysis complies with the international recommendations and guide on experimental design and analysis in pharmacology and immunopharmacology recommended by the international union of basic and clinical pharmacology (IUPHAR) [36,37] and data sharing and presentation in preclinical pharmacology [13,35]. Data are presented as mean ± S.D. or median ± IQR. Normality was tested prior to analysis with one-way ANOVA followed by Bonferroni's for multiple comparisons, where $P \leq 0.05$ was deemed significant. GraphPad Prism 10.4.2 software (San Diego, USA) was used for analysis. For *in vivo* studies, animal weight was used for randomization and group allocation to reduce unwanted sources of variations by data normalization. No animals and related *ex vivo* samples were excluded from the analysis. The study was carried out to generate groups of equal size (N = 5 of independent values) using randomization and blinded analysis.

3. Results

3.1. MIE selectively reprograms the pro-inflammatory cytokine profile of human M1 macrophages from healthy donors and IBD patients

Macrophage plasticity enables dynamic adaptation to microenvironmental cues, giving rise to distinct functional phenotypes, a process profoundly disrupted in chronic inflammatory conditions such as IBD [38]. The (classical activated) pro-inflammatory M1 phenotype, driven by IFN-γ and LPS, contributes to tissue damage, whereas the (alternatively activated) pro-resolving M2 phenotype, triggered by IL-4, facilitates resolution and repair [39]. Targeting this polarization balance represents a promising therapeutic strategy. We therefore evaluated the capacity of MIE to modulate this critical process in hMDMs from both healthy donors and IBD patients. To assess the immunomodulatory capacity of MIE, we employed a well-established *in vitro* model, as outlined in Fig. 1**A**. Briefly, monocytes were isolated from healthy donors (N = 5) and patients with IBD (N = 7), with a purity of > 95 % for $CD14^+$ cells confirmed by flow cytometry (Supplementary Figure S3). Following a 6-day differentiation with M-CSF to generate naïve macrophages (Mφ; here referred as M0), cells were polarized towards M1 or M2 phenotypes in the presence of MIE (0.1–10 μg/ml) or vehicle for 24 h. Our findings demonstrate that MIE exerts a potent and selective effect on the production of specific cytokines, namely TNF-α and IL-10. In macrophages from healthy donors, MIE treatment during M1 polarization potently suppressed TNF-α secretion in a concentration dependent manner, with a marked inhibition observed at 10 μg/ml (Fig. 1**B**). In contrast to its effects on TNF-α, MIE did not significantly alter IL-10 production in M1 macrophages at any tested concentration (Fig. 1**C**) nor in M2 macrophages, except at the highest concentration (Fig. 1**D**). In IBD derived macrophages, MIE (10 μg/ml) effectively suppressed elevated TNF-α release from M1-polarized cells (Fig. 1**E**), while sparing IL-10 production (Fig. 1**F**). Notably, MIE induced a modest but statistically significant increase in IL-10 secretion from M2 macrophages of IBD patients (Fig. 1**G**), indicating a context-dependent immunomodulatory effect.

3.2. MIE enhances monocyte adhesion and attenuates transmigration across a TNF-α-activated human endothelial barrier

The initial recruitment of circulating monocytes to sites of inflammation is a pivotal event in the initiation and perpetuation of chronic inflammation, governed by a well-characterized capture, adhesion and transmigration cascade [40]. This process is critically dependent on the activation of the vascular endothelium by pro-inflammatory cytokines like TNF-α, which upregulates adhesion molecules such as intercellular adhesion molecule-1 (ICAM-1) and vascular cell adhesion molecule-1 (VCAM-1), facilitating leukocyte adhesion and subsequent diapedesis [41]. Inhibiting this cascade represents a key therapeutic target for controlling inflammatory pathologies. Building on our compelling evidence that MIE inhibits lymphocyte trafficking [14], we turned our focus to monocytes. The experimental setup and the distinct, migratory behaviours of monocytes are summarised in Fig. 2**A**. Monocytes from healthy donors (N = 3) were pre-treated with MIE (10 μg/ml) or vehicle

for 30 min and added to TNF-α-activated HDBECs. Although MIE increased overall monocyte adhesion (Fig. 2**B**), this was secondary to its potent inhibition of transmigration (Fig. 2**C**). It did not significantly affect the percentage of monocytes undergoing the activation or spreading (phase-grey; Supplementary Figure S4). Representative images illustrate the accumulation of adherent cells and the marked reduction in transmigration (Fig. 2**D**). These findings establish that MIE limits inflammatory cell infiltration primarily by inducing monocyte adhesion and suppressing transmigration across the endothelium.

3.3. Integrated transcriptional profiling reveals NF-κB and TLR pathways as central hubs for MIE's phenotype-specific immunomodulation

To define the molecular basis of MIE's immunomodulatory effects, we performed RNA-seq on M0, M1, and M2 hMDMs treated with MIE. Global transcriptional profiles [42] (Fig. 3) revealed distinct gene expression changes across phenotypes, with (Fig. 3**A-C**) pathway enrichment visualised in radar charts. In M0 macrophages, MIE upregulated genes encoding endogenous inhibitors, including the interleukin-1 decoy receptor, interleukin 1 receptor type 2 (*IL1R2*) and the competitive antagonist, interleukin 1 receptor N antagonist (*IL1RN*), while downregulating genes encoding key mediators such as the transcriptional repressor, nuclear factor X-box binding like 1 (*NFXL1*) or the immune response marker, interferon-induced protein 44-like (*IFI44L*) (Fig. 3**A**). In the pro-inflammatory M1 phenotype, MIE robustly suppressed genes encoding key mediators, such as adrenoceptor beta 2 (*ADRB2*), poly (ADP-ribose) polymerase 11 (*PARP11*), suppressor of cytokine signalling 4 (*SOCS4*) and the immunoregulator lipoprotein lipase G (*LIPG*), resulting as the most downregulated gene, while inducing cyclin D1 gene (*CCND1*) (Fig. 3**B**). In M2 macrophages, MIE enhanced an anti-inflammatory gene expression profile, resulting in the upregulation of *IL1R2*, cluster of differentiation 40 (*CD40*), the chemokine, C-C motif chemokine ligand 17 (*CCL17*), along with the suppression of the cluster of differentiation 14 (*CD14*) (Fig. 3**C**).

Pathways analysis identified NF-κB signalling as the most consistently modulated pathway across all subsets, with phenotype specific nuances (radar charts shown in Fig. 3**A-C**). In M0 macrophages, MIE enriched genes involved in negative regulation of NF-κB (8 genes) and TLR signalling (4 genes), suggesting a primed anti-inflammatory state. In M1 macrophages, MIE exerted focused suppression of NF-κB (6 genes) and inflammatory/tissue repair pathways (6 genes), dampening the activated phenotype. In M2 macrophages, MIE induced the most extensive NF-κB reprogramming (15 genes), including 6 linked to negative feedback, reinforcing their resolving function. Supplementary Figure S5 provides full volcano plots of all DEGs related to inflammatory pathways for each phenotype. To dissect shared versus unique responses, we performed comparative analysis (Fig. 4**)**. The UpSet plot (Fig. 4**A**) revealed that MIE's transcriptional effects were highly phenotype-specific, with minimal overlap, with only one gene significantly regulated across all subsets. This underscores MIE's context-dependent precision rather than a generic anti-inflammatory effect. Bubble charts (Fig. 4**B-D**) further characterized NF-κB-related gene modulation. In M0 and M2 macrophages (Figs. 4**B** and 4**D**), MIE consistently upregulated negative regulators with the decoy receptor *IL1R2* emerging as the most significantly induced gene. In contrast, M1 macrophages showed a predominant downregulation of pro-inflammatory NF-κB targets, such as *LIPG* and *SOCS4* (Fig. 4**C**). The definitive support for both shared and phenotype-specific pathway engagement is provided in Supplementary Figure S6. In particular, Supplementary Figure S6C provides definitive quantification: M1 macrophages exhibited strong enrichment of genes linked to NF-κB, TLR, inflammasome signalling, adhesion/migration, and tissue repair. Some of these pathways were largely unaffected in M0 and M2 subsets. Together, this multi-layered transcriptomic analysis from global signatures to pathway analysis demonstrate that MIE modulates inflammatory signalling in a phenotype-specific manner. This provided the rationale for subsequent functional validation of MIE's activity across TLR pathways in primary murine peritoneal macrophages.

3.4. MIE exhibits a distinct and selective immunomodulatory profile across a broad panel of toll-like receptors (TLRs)

Building on the transcriptomic data identifying NF-κB and TLR signalling as central targets of MIE in human macrophages, we next performed functional validation using primary murine peritoneal macrophages. We first focused on the prototypical TLR4 pathway, a mediator of gram-negative bacterial inflammation and a key node in sterile inflammatory diseases [43]. To assess the temporal dynamics of MIE's action, cells were exposed to MIE (10 μg/ml) in three pharmacological contexts relative to LPS challenge: pre-treatment (30 min prior, mimicking prophylactic intervention), co-treatment (simultaneously, assessing direct interference), and post-treatment (30 min after, modelling therapeutic intervention post-inflammatory trigger) (Fig. 5**A**). This design revealed a graded pharmacodynamic profile: MIE exerted its most potent suppressive effect on LPS-induced TNF-α and IL-6 release when administered as a pre-treatment (Fig. 5**B-D**), indicating a capacity to prime macrophages towards a hypo-responsive state. A significant, though moderately attenuated inhibitory effect was consistently observed under co-treatment conditions (Fig. 5**E-G**), suggesting direct interference with early signal transduction events. Critically, a statistically significant anti-inflammatory activity was preserved even when MIE was introduced after the initial LPS stimulus (Fig. 5**H-J**). This demonstrates that MIE can disrupt an ongoing inflammatory cascade, an essential feature for therapeutic application in active disease. Having confirmed efficacy against TLR4, we next profiled MIE's activity across a broader panel of TLRs. Macrophages were pre-treated with MIE and stimulated with specific agonists for TLR2–9. The detailed cytokine secretion profiles (TNF-α, IL-6, PGE_2) for each TLR agonist are comprehensively detailed in Supplementary Figure S7A-**F**. Analysis of this dataset revealed a striking and highly specific pattern of immunomodulation: MIE potently blunted the inflammatory response triggered by TLR2, TLR4, and TLR6, yet exhibited minimal to no modulating effect on signalling driven by TLR3, TLR5, TLR7, and TLR9. This specificity positions MIE not as a broad-spectrum TLR inhibitor, but as a precision immunomodulator that selectively targets inflammatory TLR subsets. By preserving antiviral and antibacterial signalling pathways [44], MIE offers a refined therapeutic strategy with potential for improved safety and efficacy.

3.5. MIE's selective TLR4 inhibition impinges on the MyD88/NF-κB signalling axis

The selective suppression of TLR2/4/6 by MIE prompted investigation into shared signalling mechanisms underlying this specificity. We hypothesised that MIE acts on a common node within the MyD88-dependent pathway, which converges on NF-kB activation. To test this, primary murine peritoneal macrophages were pre-treated with MIE and challenged with specific TLR agonists (Fig. 6**A)**. Polar chart analysis (Fig. 6**B**) confirmed MIE's strongest inhibitory effect on TLR4, with selective activity across the TLR2/4/6 cluster and sparing of other TLRs. We first assessed downstream cytokine output. MIE pre-treatment significantly suppressed TNF-α, IL-6, and PGE_2 secretion in LPS-stimulated macrophages (Fig. 6**C**), consistent with NF-κB pathway inhibition. We then examined upstream signalling events: western blot analysis revealed that MIE attenuated LPS-induced TLR4 expression (Fig. 6**D**) and upregulation of MyD88 and total NF-κB p65 protein level (Fig. 6**F**). Densitometric quantification across three biological replicates confirmed significant reductions in protein levels (Figs. 6**E,** 6**G and** 6**H**). The specificity and reproducibility of these immunoblotting results are robustly corroborated by the full, uncropped western blot images presented in **Original western blot file**. In summary, this multi-tiered mechanistic investigation, progressing from cellular output to

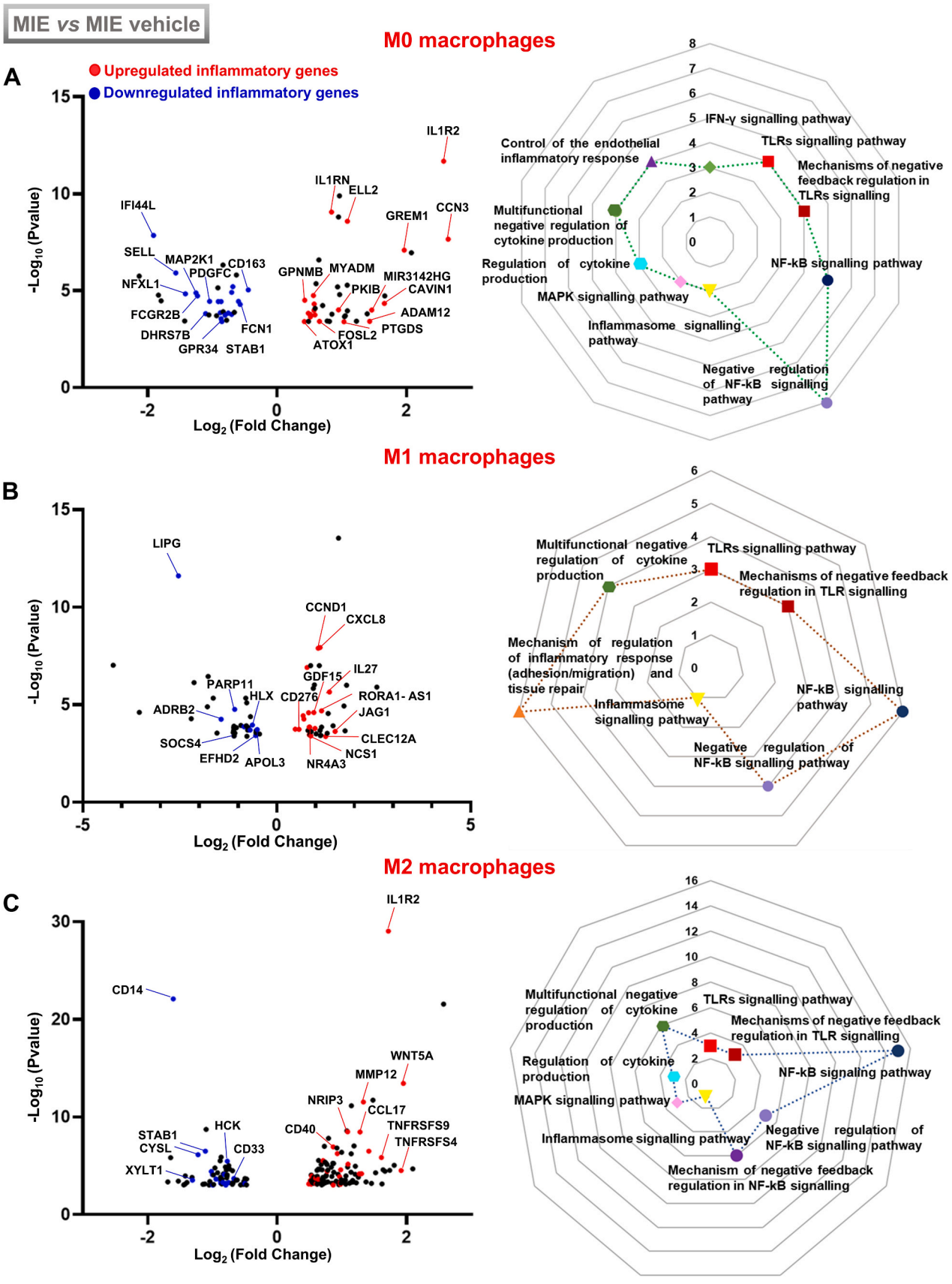

(caption on next page)

Fig. 3. Gene expression profiling identifies NF-κB as the key regulator of inflammatory pathway activation in human polarized macrophages. Volcano plots (**A-C**) show differentially expressed genes (DEGs) across naïve macrophages (Mφ; also called M0), M1 and M2 macrophage phenotypes in MIE *vs* MIE vehicle comparison. The plot shows the Fold-Change on the X-axis versus the unadjusted *P* values (on a -Log_{10} scale) on the Y-axis. The X-axis indicates the average expression level for each gene. Red and blue circles denote significantly up- and down-regulated inflammatory-related genes, respectively. Radar charts illustrate the enrichment of key inflammatory signalling pathways (the corresponding volcano plots are reported in Supplementary Fig. S5A-**C**) for each phenotype. The NF-κB signalling pathway is the most prominently modulated pathway across all macrophage polarization states (M0, M1 and M2). Pathway-specific gene counts: M0 phenotype (**A**): Negative regulation of NF-κB (8 genes), NF-κB signalling (5), control of endothelial inflammatory response (4), negative regulation of cytokine production (4), negative feedback in TLR signalling (4), TLR signalling (4), regulation of cytokine production (3), IFN-γ signalling (3), inflammasome signalling (2), MAPK signalling (2). M1 phenotype (**B**): NF-κB signalling (6), inflammatory response & tissue repair (6), negative regulation of NF-κB (4), negative regulation of cytokine production (4), TLR signalling (3), negative feedback in TLR signalling (3), inflammasome signalling (1). M2 phenotype (**C**): NF-κB signalling (15), negative feedback in NF-κB signalling (6), negative regulation of cytokine production (6), negative regulation of NF-κB (5), negative feedback in TLR signalling (3), TLR signalling (3), regulation of cytokine production (3), MAPK signalling (3), inflammasome signalling (1).

proximal signalling events, definitively identifies the MyD88/NF-κB axis as a primary target of MIE on TLR4. These data provide a coherent molecular explanation for the observed transcriptomic and functional phenotypes, demonstrating that MIE blunts the pro-inflammatory response by strategically impinging upon this core signalling pathway, thereby providing a mechanistic rationale for its selective modulation of a defined subset of TLR signalling pathways [11,44].

4. Discussion

This study uncovers a previously unrecognized facet of MIE's immunomodulatory profile, identifying it as a master regulator of early innate immune responses. MIE operates through a multi-tiered mechanism: systemically, it restricts monocyte recruitment to inflamed tissues, and locally, it acts as a molecular rheostat to reprogram macrophage polarization and function. Crucially, this is achieved not via broad immunosuppression, but through selective modulation of TLR2/4/6 activity, TLR4 expression and their upstream adaptor MyD88 and downstream trascriptional factor NF-κB. This targeted strategy offers a refined approach to resolving chronic inflammation while preserving essential host defense [1].

The initiation of inflammation begins with leukocyte extravasation, a process reliant on monocyte adhesion and migration on activated endothelium, via adhesion molecules including ICAM-1 and VCAM-1 [45]. Our finding that MIE enhances monocyte adhesion while inhibiting transmigration identifies a critical upstream mechanism contributing to its *in vivo* efficacy [8].

Mechanistically, this apparent paradox can be reconciled by considering that firm adhesion is necessary but not sufficient for diapedesis. Transmigration requires additional signals, including integrin inside-out activation, cytoskeletal remodelling, and endothelial junctional opening. Several studies have shown that stimuli can increase adhesion yet impair transmigration by selectively modulating these downstream steps. For example, short-term LPS stimulation enhances monocyte adhesion but markedly reduces transendothelial migration under static conditions [46]. Similarly, mechanical forces at the endothelial interface regulate cytoskeletal tension and junctional dynamics, meaning that adhesion can be stabilized without permitting junctional penetration [47]. Our data suggest that MIE may act at this checkpoint: promoting integrin-mediated adhesion while interfering with cytoskeletal reorganization or endothelial junctional changes required for diapedesis. This differential regulation of sequential steps in the extravasation cascade provides a plausible explanation for the observed phenotype, consistent with broader models of leukocyte trafficking [8,48].

Functionally, prolonged adhesion without transmigration may sequester monocytes at the vascular interface, reducing their infiltration into tissues and thereby limiting chronic inflammatory drivers. At the same time, sustained adhesion could trigger local endothelial signalling that reinforces vascular stability. Thus, rather than being pro-inflammatory, this uncoupling of adhesion from transmigration may represent a protective mechanism that dampens tissue infiltration while modulating vascular homeostasis [49]. Such a mechanism is particularly relevant in conditions such as IBD and atherosclerosis, where excessive monocyte entry into tissues drives chronic inflammation.

Once in the tissue, monocytes differentiate into macrophages, whose polarisation into pro-inflammatory (M1) or pro-resolving (M2) phenotypes is tightly regulated but often disrupted in chronic inflammation [5]. Our findings demonstrate that MIE possesses a selective and potentially therapeutic immunomodulatory capacity, capable of reprogramming the dysfunctional cytokine profile of human macrophages derived from both healthy donors and patients with IBD. The study specifically reveals that MIE potently and concentration-dependently suppresses the secretion of the pro-inflammatory cytokine TNF-α during M1 macrophage polarization, a key driver of tissue damage in chronic inflammation [50,51]. Critically, this effect was observed in macrophages from healthy donors and was particularly pronounced in cells from IBD patients, where TNF-α levels are pathologically elevated [52]. In contrast, MIE did not significantly inhibit the production of the anti-inflammatory cytokine IL-10 in M1 macrophages from either group, preserving a crucial endogenous regulatory mechanism. The differential effect of MIE on IL-10 secretion, showing no change in M1 macrophages but a modest, statistically significant enhancement in M2 macrophages from IBD patients, highlights a potential context-dependent and phenotype-specific immunomodulatory action. This selective reprogramming suggests MIE's potential to correct the polarization imbalance central to IBD pathology, shifting the macrophage functional state from a pro-inflammatory to a pro-resolving phenotype [6].

Elevated baseline IL-10 levels in macrophages from IBD patients are consistent with reports of compensatory anti-inflammatory cytokine production during chronic inflammation [53,54]. This context is crucial for interpreting MIE's differential effects. As supported by the literature, IL-10 in M1 macrophages is often co-expressed with pro-inflammatory mediators such as TNF-α and IL-6, which may limit its net anti-inflammatory impact within this inflammatory milieu [55]. In contrast, M2 macrophages are transcriptionally primed to amplify regulatory pathways [56]. Therefore, MIE's specific enhancement of IL-10 secretion in M2 macrophages, but not in M1 cells, likely reflects and reinforces the distinct transcriptional programs of these subsets.

Functionally, this divergence could critically shape the inflammatory environment in IBD. In M1 macrophages, the failure of MIE to further elevate IL-10, against a backdrop of suppressed TNF-α, may still permit pro-inflammatory signalling to persist. Conversely, in M2 macrophages, the compound's ability to boost IL-10 may potentiate resolution pathways, further dampen immune activation and promote epithelial repair [57]. Moreover, IL-10 has been shown to reprogram macrophage metabolism toward oxidative phosphorylation, thereby stabilizing anti-inflammatory functions [58]. Thus, MIE's strategy of selectively augmenting IL-10 in the regulatory M2 subset may effectively tilt the balance toward tissue repair, even within the complex cytokine landscape of IBD. This mechanistic insight, limiting a key pathogenic driver while selectively reinforcing a regulatory axis, helps explain the extract's overall anti-inflammatory efficacy and positions it as a promising agent for modulating macrophage plasticity in IBD and inflammatory-based diseases [59] and distinguishes MIE from broad immunosuppressants

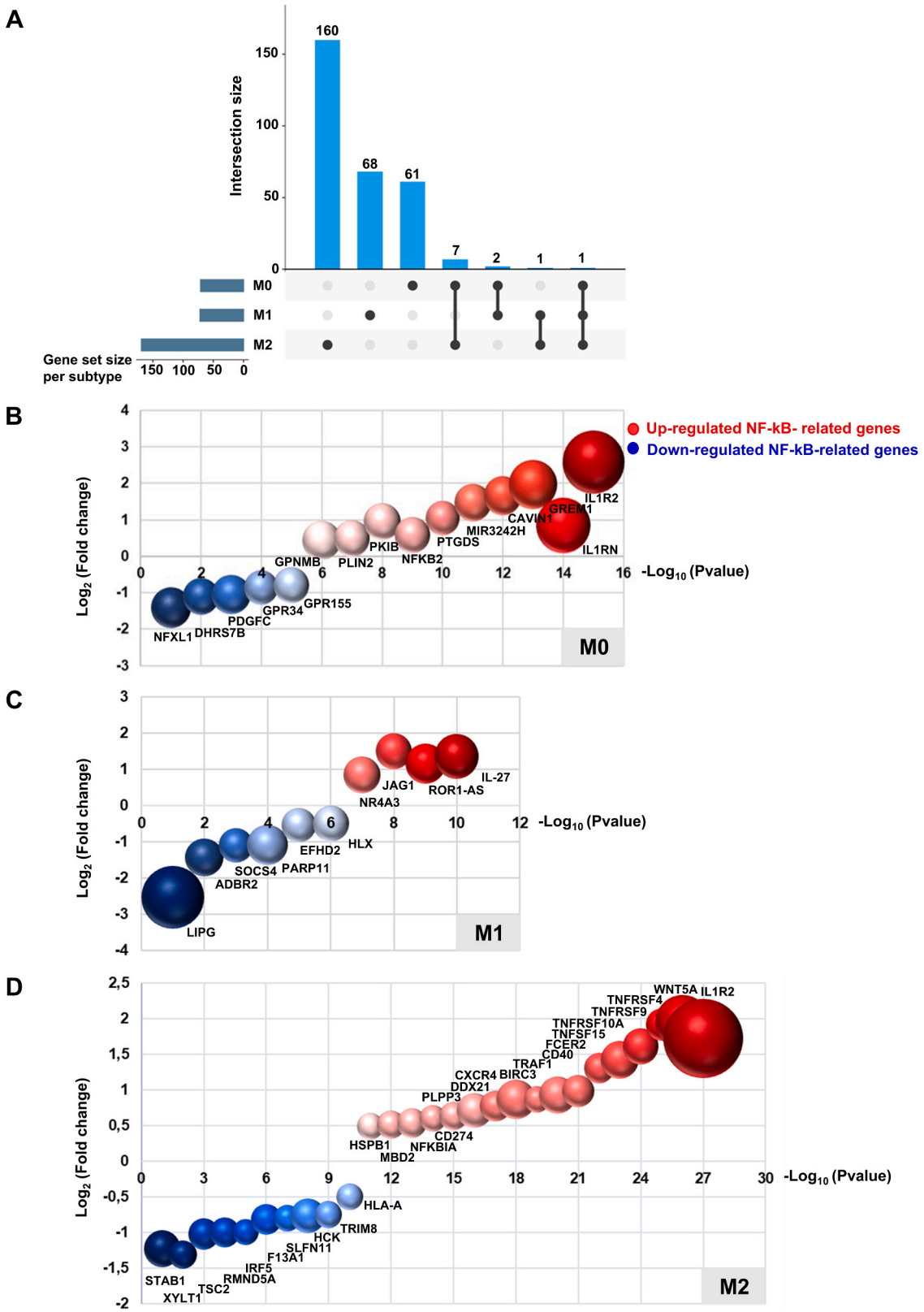

Fig. 4. Comparative transcriptomic analysis of macrophage phenotypes highlights unique and common NF-κB signatures. UpSet plot (**A**) shows distinct and overlapping genes across main macrophage subtypes (M0, M1 and M2). Vertical bars show the number of common genes between M0, M1 and M2 phenotypes (intersection size). Horizontal bars illustrate the total number of genes (set size). Bubble charts (**B**-**D**) show the most up-regulated (red) and down-regulated NF-κB related genes (blue) in M0 (**B**), M1 (**C**) and M2 (**D**) macrophages. The X-axis corresponds to -Log_{10} (*P*value) while Y-axis indicates the Log_2 (Fold change). The bubble size represents the number of significant genes for a given enriched term. The colour intensity corresponds to the enrichment significance, with red indicating a higher -Log_{10}(*P*value) and blue indicating a lower -Log_{10}(*P*value).

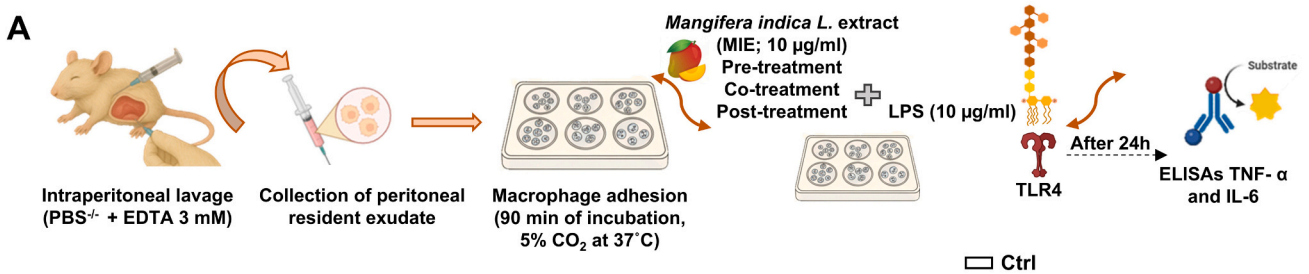

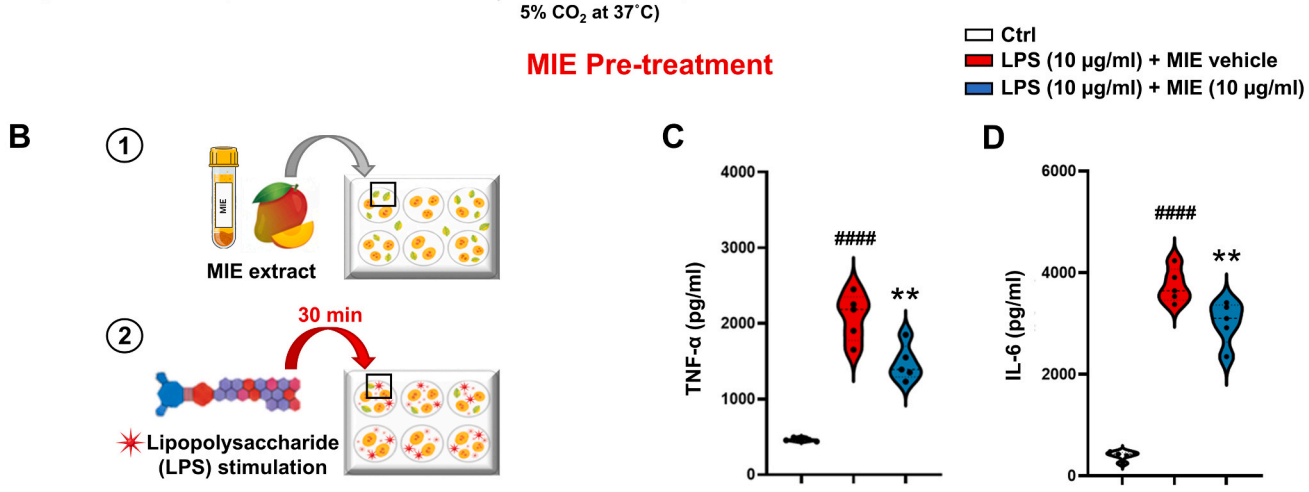

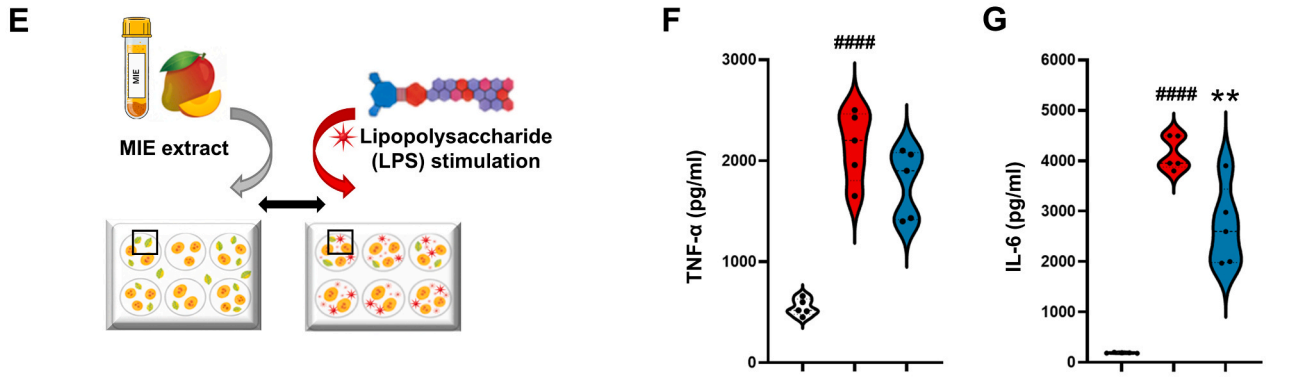

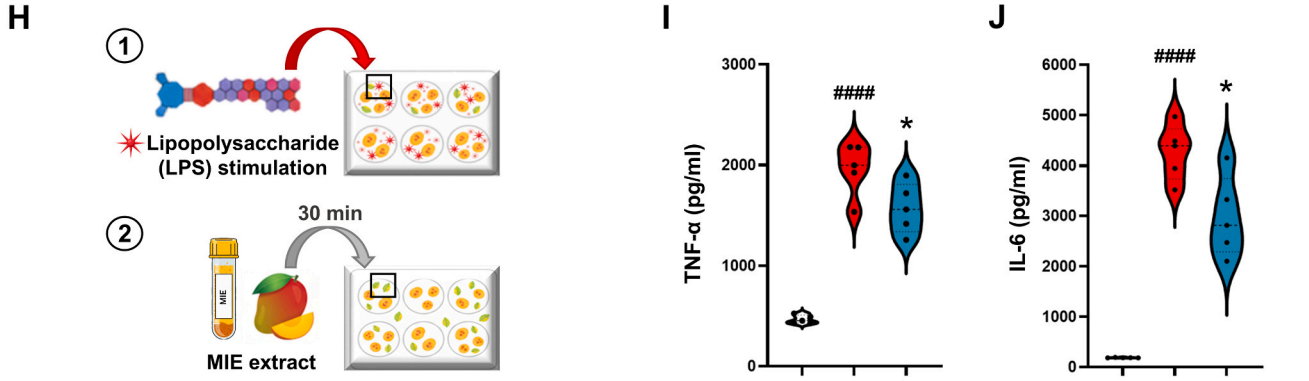

(caption on next page)

Fig. 5. Temporal profiling of MIE shows differential modulation of LPS-induced cytokine responses in peritoneal macrophages. Schematic representation of the experimental workflow (**A**). Resident peritoneal exudate cells were collected from C57BL/6 J wild type (WT) mice by intraperitoneal (i.p.) lavage. After adherence, macrophages were treated with MIE extract (10 μg/ml) or vehicle (DMSO, 0.067 %) according to three temporal regimens relative to LPS (10 μg/ml) stimulation (**A**): pre-treatment (30 min before LPS, **B**), co-treatment (simultaneous with LPS, **E**), and post-treatment (30 min after LPS, **H**). After 24 h of incubation, culture supernatants were collected and analyzed by ELISA assays to quantify TNF-α and IL-6 levels. Graphs show cytokine concentrations for each treatment condition: TNF-α (**C**, **F**, **I**) and IL-6 (**D**, **G**, **J**) in pre-, co-, and post-treatment settings, respectively. Data are expressed as pg/ml and presented as violin plot of N = 5 mice per group. Statistical analysis was conducted by one-way ANOVA followed by Bonferroni's for multiple comparisons. $^{\#\#\#\#}P \leq 0.0001$ *vs* Ctrl; $^{*}P \leq 0.05$, $^{**}P \leq 0.01$ *vs* LPS + MIE vehicle.

that carry an increased risk of infection [6]. Transcriptomic profiling revealed that MIE's effects are highly phenotype-specific, with pronounced modulation of genes involved in NF-κB, TLR, inflammasome signalling pathways, as well as mechanisms regulating inflammatory response (adhesion/migration) and tissue repair. This gene signature pointed to the TLRs system as a primary target, consistent with the central role in macrophage activation [2].

Our most significant finding is the identification of MIE as a broad TLR2/4/6 signalling rheostat to attenuate MyD88/NF-κB-driven inflammation. Functional profiling across TLR agonists revealed potent inhibition of TLR2, TLR4, and TLR6, while sparing TLR3, TLR5, TLR7, and TLR9. This specificity has important therapeutic implications: the TLR2/4/6 cluster responds to bacterial components [e.g., lipoproteins, LPS, Macrophage-Activating Lipopeptide-2 (MALP-2)] and Damage-Associated Molecular Patterns (DAMPs), key drivers of the sterile inflammation in chronic diseases such as IBD, rheumatoid arthritis, and metabolic syndrome [60]. In contrast, the unaffected TLRs are crucial for antiviral immunity (TLR3, TLR7, TLR9) and flagellin recognition (TLR5) [61]. By preserving these pathways, MIE may offer a superior safety profile compared to broad-acting biologics like anti-TNF therapies [8].

Mechanistically, MIE's selective modulation maps on to the MyD88/NF-κB axis. It modulates TLR4, MyD88 and total NF-κB p65 protein expression, explaining the coordinated downregulation of NF-κB target genes observed in our transcriptomic and cytokine data [62]. While the precise molecular target upstream remains to be defined, our findings suggest MIE interferes with early events TLR2/4/6 signalling, such as receptor complex formation, or adapters protein recruitment. This targeted disruption of shared signalling hub enables broad anti-inflammatory effects without indiscriminate pathway suppression, aligning with emerging strategies for pathway-specific immunomodulation [6]. Notably, MIE retains efficacy even when administered after inflammatory stimulation, supporting its therapeutic use in established disease. Beyond acute inflammation, our data raises the possibility that MIE may influence trained immunity, a form of innate memory driven by epigenetic and metabolic reprogramming [2]. The sustained modulation of NF-κB and metabolic pathways suggests that MIE could reset hyperactive innate immune states, potentially preventing disease flares in chronic conditions. This dual capacity, acute cytokine suppression and long-term innate immune reprogramming, warrants further investigation in models of trained immunity [1].

Taken together with our previous work on MIE's effects on adaptive immunity and the neuro-immune axis [3,15], these findings complete a comprehensive mechanistic framework. MIE emerges as a multi-targeted agent capable of dampening early innate triggers (monocyte recruitment, TLR expression and signalling), reshaping the inflammatory microenvironment (macrophage polarization), and resolving the associated adaptive and neurological sequelae of chronic inflammation. This integrated, multi-pathway mode of action is especially compelling for complex, multifactorial diseases such as IBD. Here, MIE's potential as a scientifically substantiated nutraceutical or novel food ingredient could offer a realistic, evidence-based complementary strategy to modulate the convergent pathogenic networks driving disease pathology.

5. Conclusions and study limitations

In conclusion, this study systematically deciphers the multi-faceted mechanism of action of MIE, positioning it as a precision immunomodulator that intervenes at critical junctures of the inflammatory cascade. We establish that MIE operates from the systemic level, by inhibiting monocyte recruitment, to the molecular level, where it functions as a selective rheostat of innate immunity by specifically modulating the TLR4-MyD88-NF-κB axis. This targeted mechanism, which preserves other critical TLR pathways and subtly reinforces anti-inflammatory programs in macrophages, distinguishes MIE from broad suppression immunosuppressants and underscores its potential as a sophisticated therapeutic agent with a predictably superior safety profile.

While our findings provide a robust mechanistic framework, certain limitations highlight avenues for future research. First, the functional validation of TLRs selectivity was conducted in murine macrophages. Although the core TLR signalling machinery is evolutionarily conserved, direct confirmation of this selective inhibition in primary human macrophages would strengthen the translational relevance of our findings. Second, the *in vivo* functional consequence of this specific TLR modulation, while strongly inferred from our data, requires definitive validation using TLR-pathway specific disease models. Third, the long-term impact of MIE on antimicrobial host defence, despite its sparing of key antiviral TLRs, remains to be fully elucidated in integrated immunological challenge models. Finally, a limitation to the generalisability of the study is that it did not consider gender/sex issues.

Notwithstanding these limitations, our work provides a compelling preclinical rationale for the continued development of MIE. Its unique integrated strategy, simultaneously targeting leukocyte trafficking, macrophage programming, and specific pro-inflammatory signalling, represents a paradigm shift from non-specific immunosuppression towards re-establishing innate immune homeostasis in complex chronic inflammatory diseases by nutraceuticals and/or novel food ingredient/s.

CRediT authorship contribution statement

Areeba Fatima: Investigation, Formal analysis, Data curation. **Jenefa Begum:** Investigation, Formal analysis, Data curation. **Erika Esposito:** Investigation, Formal analysis, Data curation. **Francesco Maione:** Writing – review & editing, Writing – original draft, Supervision, Project administration. **Martina Smimmo:** Investigation, Formal analysis, Data curation. **Alyssa M Urbanowski:** Investigation, Formal analysis, Data curation. **Amnah M Khormi:** Investigation, Formal analysis, Data curation. **Christopher Mahony:** Formal analysis, Data curation. **Asif Jilani Iqbal:** Writing – review & editing, Writing – original draft, Supervision, Formal analysis, Conceptualization. **Noemi Marigliano:** Investigation, Formal analysis, Data curation. **Helen M McGettrick:** Writing – review & editing, Writing – original draft, Supervision. **Anella Saviano:** Writing – review & editing, Writing – original draft, Investigation, Formal analysis, Data curation, Conceptualization. **Tariq H Iqbal:** Investigation, Formal analysis, Data curation. **Anna Schettino:** Writing – original draft, Visualization, Methodology, Investigation, Formal analysis, Data curation, Conceptualization. **Adel Abo Mansour:** Investigation, Formal analysis, Data curation.

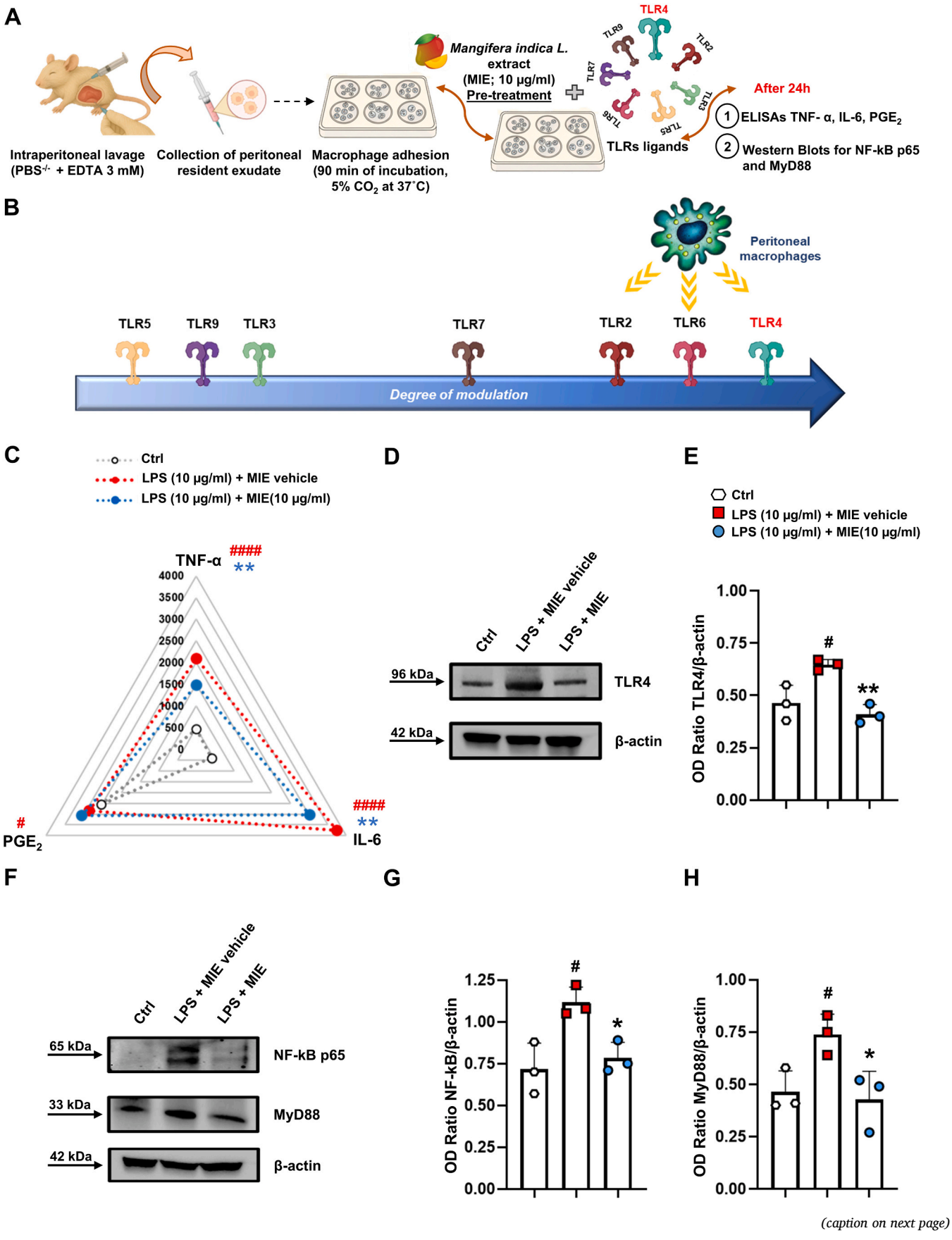

(caption on next page)

Fig. 6. MIE selectively targets TLR4 in peritoneal macrophages, modulating pro-inflammatory signalling through the MyD88/NF-κB axis. Schematic overview of the experimental workflow (**A**). Resident peritoneal exudate cells were collected from C57BL/6 J wild type (WT) mice via intraperitoneal (i.p.) lavage. After adhesion, macrophages were pre-treated with MIE extract (10 μg/ml) or vehicle (DMSO, 0.067 %) for 30 min, followed by stimulation with specific agonists for TLR2, TLR3, TLR4, TLR5, TLR6, TLR7, or TLR9 for 24 h (**A**). Panel **B** summarizes the effects of MIE across the different TLRs, with detailed charts provided in Supplementary Fig. S7A-**F**. The data depict the relative activity of MIE on each TLR, highlighting preferential activation of TLR4, moderate modulation of TLR2 and TLR6, and minimal effects on TLR3, TLR5, TLR7 and TLR9 (**B**). Radar chart analysis (**C**) illustrates cytokine secretion patterns in LPS (10 μg/ml)-stimulated macrophages. ELISA assays were performed to measure TNF-α, IL-6 and PGE_2 levels under the experimental conditions (**C**). $^{\#}P \leq 0.05$, $^{\#\#\#\#}P \leq 0.0001$ *vs* Ctrl; $^{**}P \leq 0.01$ *vs* LPS + MIE vehicle. Cell pellet lysates from all experimental conditions were analyzed by western blot to investigate the TLR4 signalling pathway, assessing the expression of TLR4 (~96 kDa), MyD88 (~33 kDa) and total NF-κB p65 (~65 kDa), representing the initiating receptor, adaptor protein and key downstream effector of TLR4 activation, respectively. Representative western blot images are shown from three independent experiments with similar results (**D** and **F**). Cumulative densitometric values (**E, G** and **H**) are expressed as OD ratio with β-actin. Values are presented as means ± S.D. of N = 3 independent experiments. Statistical analysis was conducted by one-way ANOVA followed by Bonferroni's for multiple comparisons. $^{\#}P \leq 0.05$ *vs* Ctrl; $^{*}P \leq 0.05$, $^{**}P \leq 0.01$ *vs* LPS + MIE vehicle.

Ethics approval and consent to participate

Human studies were approved by the University of Birmingham Local Ethical Review Committee (ERN_18–0382: Healthy Blood Donor Collection; 21/PR/0515: Exploration and validation of host and microbial biomarkers in newly diagnosed patients with immune-mediated inflammatory disease of the gastrointestinal tract [IMGID-INCEPTION]; IRAS: 287279; Protocol number: RG_21–009).

Written informed consent was obtained from all participants prior to inclusion in the study. The study was conducted in accordance with recognized ethical standards, including the Declaration of Helsinki, the US Federal Policy for the Protection of Human Subjects, and the European Medicines Agency Guidelines for Good Clinical Practice.

In vivo experiments were performed in accordance with UK legislation (Animal Scientific Procedures Act 1986) under the authority of the UK Home Office license PPL P50CB9C61: Leukocyte recruitment and retention in acute and chronic inflammation, with approval from the University of Birmingham Local Ethical Review Committee. All animal experiments were conducted in compliance with the ARRIVE (Animal Research: Reporting of *In Vivo* Experiments) guidelines. The study also adhered to the WMA Statement on Animal Use in Biomedical Research and the European Union Directive 2010/63/EU on the protection of animals used for scientific purposes, ensuring internationally recognized standards for experimental design, animal welfare, and pharmacological care.

Declaration of Generative AI and AI-assisted technologies in the writing process

During the preparation of this work the authors used ChatGPT and DeepSeek only to revise and/or double-check English language and syntax. After using these tools, Authors reviewed and edited the content as needed and for full intellectual property.

Funding

This study was supported by internal funding of *ImmunoPharmaLab*, Department of Pharmacy, University of Naples, Federico II. AAM extends his appreciation to the Deanship of Research and Graduate Studies at King Khalid University for funding this work through the "Small Research Project" under grant number RGP.1/82/46. ASch is supported by University of Naples Federico II PhD scholarship in "Nutraceuticals, functional foods and human health" (PNRR DM 118 M4C1– INV 4.1 ricerca PNRR generici). NM is supported by AORN A. Cardarelli Scholarship (n. 725/2022 GRC- Linea Progettuale 1.3: "Gestione delle cronicità"). ASav is supported by RTD-A research contract for the thematic spoke "Validating acid nucleic-based drugs using *in vitro* and *in vivo* models of cancer and immune-related diseases". The research activity is focused on topics of interest for the Department of Pharmacy, Federico II, included in the grant application marked MUR identification code CN00000041 "National Center for Gene Therapy and Drugs based on RNA Technology" (initiative financed by the European Union – NextGenerationEU and Funding granted with Directorial Decree n.1035 of 06.17.2022 under PNRR MUR – M4C2 – Investment 1.4- CUP UNINA: E63C22000940007). AJI supported BHF Project grant PG/23/11476 and Birmingham Fellowship. Part of this research was carried out at the National Institute for Health and Care Research (NIHR) Birmingham Biomedical Research Centre (BRC).

Declaration of Competing Interest

We wish to confirm that there are no known conflicts of interest associated with this publication and there has been no significant financial support for this work that could have influenced its outcome. We confirm that the manuscript has been read and approved by all named authors and that there are no other persons who satisfied the criteria for authorship but are not listed.

We further confirm that the order of authors listed in the manuscript has been approved by all of us. We confirm that we have given due consideration to the protection of intellectual property associated with this work and that there are no impediments to publication, including the timing of publication, with respect to intellectual property. In so doing we confirm that we have followed the regulations of our institutions concerning intellectual property.

We further confirm that all aspects of this work involving animal experimentation or clinical ex vivo data were performed with the appropriate ethical approvals from all relevant bodies. These approvals are stated and acknowledged within the manuscript.

The Corresponding Author is the sole contact for the Editorial process, including communications via Editorial Manager and with the journal office. They are responsible for keeping all co-authors informed of the manuscript's progress, revisions, and for obtaining their final approval of the proofs.

Appendix A. Supporting information

Supplementary data associated with this article can be found in the online version at doi:10.1016/j.phrs.2026.108099.

Data Availability

All data generated or analyzed during this study are included in this published article and its supplementary information files. Reagents and unique biological resources developed in this study are available from the corresponding author upon reasonable request. Such requests will be fulfilled contingent upon the completion of a formal Material Transfer Agreement (MTA) with *ImmunoPharmaLab* at the Department of Pharmacy, University of Naples Federico II, which retains ownership of these materials. Please note that we do not see the necessity to share raw data via a Research Elements Journal.

References

[1] M. Divangahi, P. Aaby, S.A. Khader, L.B. Barreiro, S. Bekkering, T. Chavakis, R. van Crevel, N. Curtis, A.R. DiNardo, J. Dominguez-Andres, R. Duivenvoorden, S. Fanucchi, Z. Fayad, E. Fuchs, M. Hamon, K.L. Jeffrey, N. Khan, L.A.B. Joosten, E. Kaufmann, E. Latz, G. Matarese, J.W.M. van der Meer, M. Mhlanga, S. Moorlag,

W.J.M. Mulder, S. Naik, B. Novakovic, L. O'Neill, J. Ochando, K. Ozato, N. P. Riksen, R. Sauerwein, E.R. Sherwood, A. Schlitzer, J.L. Schultze, M.H. Sieweke, C.S. Benn, H. Stunnenberg, J. Sun, F.L. van de Veerdonk, S. Weis, D.L. Williams, R. Xavier, M.G. Netea, Trained immunity, tolerance, priming and differentiation: distinct immunological processes, Nat. Immunol. 22 (1) (2021) 2–6.

[2] M.G. Netea, J. Domínguez-Andrés, L.B. Barreiro, T. Chavakis, M. Divangahi, E. Fuchs, L.A.B. Joosten, J.W.M. van der Meer, M.M. Mhlanga, W.J.M. Mulder, N. P. Riksen, A. Schlitzer, J.L. Schultze, C. Stabell Benn, J.C. Sun, R.J. Xavier, E. Latz, Defining trained immunity and its role in health and disease, Nat. Rev. Immunol. 20 (6) (2020) 375–388.

[3] C. Yunna, H. Mengru, W. Lei, C. Weidong, Macrophage M1/M2 polarization, Eur. J. Pharm. 877 (2020) 173090.

[4] Y. Yao, X.H. Xu, L. Jin, Macrophage polarization in physiological and pathological pregnancy, Front Immunol. 10 (2019) 792.

[5] P.J. Murray, T.A. Wynn, Protective and pathogenic functions of macrophage subsets, Nat. Rev. Immunol. 11 (11) (2011) 723–737.

[6] T.A. Wynn, K.M. Vannella, Macrophages in tissue repair, regeneration, and fibrosis, Immunity 44 (3) (2016) 450–462.

[7] E. Diez-Martin, L. Hernandez-Suarez, C. Muñoz-Villafranca, L. Martin-Souto, E. Astigarraga, A. Ramirez-Garcia, G. Barreda-Gómez, Inflammatory bowel disease: a comprehensive analysis of molecular bases, predictive biomarkers, diagnostic methods, and therapeutic options, Int. J. Mol. Sci. 25 (13) (2024).

[8] K. Ley, C. Laudanna, M.I. Cybulsky, S. Nourshargh, Getting to the site of inflammation: the leukocyte adhesion cascade updated, Nat. Rev. Immunol. 7 (9) (2007) 678–689.

[9] M. Xue, B.V. Atallah, M. Scanziani, Equalizing excitation-inhibition ratios across visual cortical neurons, Nature 511 (7511) (2014) 596–600.

[10] T. Dubovik, M. Lukačišin, E. Starosvetsky, B. LeRoy, R. Normand, Y. Admon, A. Alpert, Y. Ofran, M. G'Sell, S.S. Shen-Orr, Interactions between immune cell types facilitate the evolution of immune traits, Nature 632 (8024) (2024) 350–356.

[11] T. Kawasaki, T. Kawai, Toll-like receptor signaling pathways, Front Immunol. 5 (2014) 461.

[12] M. Imran, M.S. Arshad, M.S. Butt, J.H. Kwon, M.U. Arshad, M.T. Sultan, Mangiferin: a natural miracle bioactive compound against lifestyle related disorders, Lipids Health Dis. 16 (1) (2017) 84.

[13] A. Saviano, F. Raucci, G.M. Casillo, A.A. Mansour, V. Piccolo, C. Montesano, M. Smimmo, V. Vellecco, G. Capasso, A. Boscaino, V. Summa, N. Mascolo, A. J. Iqbal, R. Sorrentino, R. d'Emmanuele, di Villa Bianca, M. Bucci, V. Brancaleone, F. Maione, Anti-inflammatory and immunomodulatory activity of Mangifera indica L. reveals the modulation of COX-2/mPGES-1 axis and Th17/Treg ratio, Pharm. Res. 182 (2022) 106283.

[14] A. Saviano, A. Schettino, N. Iaccarino, A.A. Mansour, J. Begum, N. Marigliano, F. Raucci, F. Romano, G. Riccardi, E. Mitidieri, R. d'Emmanuele di Villa Bianca, I. Bello, E. Panza, M. Smimmo, V. Vellecco, P. Rimmer, J. Cheesbrough, Z. Zhi, T. H. Iqbal, S. Pieretti, V.M. D'Amore, L. Marinelli, V. La Pietra, R. Sorrentino, L. Costa, F. Caso, R. Scarpa, G. Cirino, A. Randazzo, M. Bucci, H.M. McGettrick, A. J. Iqbal, F. Maione, A reverse translational approach reveals the protective roles of Mangifera indica in inflammatory bowel disease, J. Autoimmun. 144 (2024) 103181.

[15] E. Lucarini, A. Schettino, N. Marigliano, C. Ciampi, M. Smimmo, F. Romano, A. Paolillo, L. Izzo, J. Begum, A.A. Mansour, N. Iaccarino, A. Randazzo, K.V. Greco, R. Scarpa, F. Caso, A.J. Iqbal, M. Bucci, C. Ghelardini, L.D.C. Mannelli, A. Saviano, F. Maione, Exploring the dual role of Mangifera indica L. in regulating immune response and pain persistence in inflammatory bowel disease, Pharm. Res. 217 (2025) 107773.

[16] M. Nahrendorf, F.K. Swirski, E. Aikawa, L. Stangenberg, T. Wurdinger, J. L. Figueiredo, P. Libby, R. Weissleder, M.J. Pittet, The healing myocardium sequentially mobilizes two monocyte subsets with divergent and complementary functions, J. Exp. Med. 204 (12) (2007) 3037–3047.

[17] A. Saviano, A.A. Manosour, F. Raucci, F. Merlino, N. Marigliano, A. Schettino, M. Wahid, J. Begum, A. Filer, J.E. Manning, G.M. Casillo, M. Piccolo, M.G. Ferraro, S. Marzano, P. Russomanno, R. Bellavita, C. Irace, J. Amato, M. Alfaifi, P. Rimmer, T. Iqbal, S. Pieretti, V. Vellecco, F. Caso, L. Costa, R. Giacomelli, R. Scarpa, G. Cirino, M. Bucci, H.M. McGettrick, P. Grieco, A.J. Iqbal, F. Maione, New biologic (Ab-IPL-IL-17) for IL-17-mediated diseases: identification of the bioactive sequence (nIL-17) for IL-17A/F function, Ann. Rheum. Dis. 82 (11) (2023) 1415–1428.

[18] E.M. Sturm, B. Radnai, K. Jandl, A. Stančić, G.P. Parzmair, C. Högenauer, P. Kump, H. Wenzl, W. Petritsch, T.R. Pieber, R. Schuligoi, G. Marsche, N. Ferreirós, A. Heinemann, R. Schicho, Opposing roles of prostaglandin D2 receptors in ulcerative colitis, J. Immunol. 193 (2) (2014) 827–839.

[19] F. Krautter, C. Recio, M.T. Hussain, D.R. Lezama, F. Maione, M. Chimen, A.J. Iqbal, Characterisation of endogenous Galectin-1 and -9 expression in monocyte and macrophage subsets under resting and inflammatory conditions, Biomed. Pharm. 130 (2020) 110595.

[20] Y. Wang, W. Smith, D. Hao, B. He, L. Kong, M1 and M2 macrophage polarization and potentially therapeutic naturally occurring compounds, Int. Immunopharmacol. 70 (2019) 459–466.

[21] S. Gordon, F.O. Martinez, Alternative activation of macrophages: mechanism and functions, Immunity 32 (5) (2010) 593–604.

[22] L. Wang, T.G. Oh, J. Magida, G. Estepa, S.M.B. Obayomi, L.-W. Chong, J. Gatchalian, R.T. Yu, A.R. Atkins, D. Hargreaves, M. Downes, Z. Wei, R.M. Evans, Bromodomain containing 9 (BRD9) regulates macrophage inflammatory responses by potentiating glucocorticoid receptor activity, Proc. Natl. Acad. Sci. 118 (35) (2021) e2109517118.

[23] N.S. Ahmed, J. Gatchalian, J. Ho, M.J. Burns, N. Hah, Z. Wei, M. Downes, R. M. Evans, D.C. Hargreaves, BRD9 regulates interferon-stimulated genes during macrophage activation via cooperation with BET protein BRD4, Proc. Natl. Acad. Sci. 119 (1) (2022) e2110812119.

[24] A. Sodhi, S. Tarang, V. Kesherwani, Concanavalin A induced expression of Toll-like receptors in murine peritoneal macrophages, Int. Immunopharmacol. 7 (2007) 454–463.

[25] P.A. Louwe, L. Badiola Gomez, H. Webster, G. Perona-Wright, C.C. Bain, S. J. Forbes, S.J. Jenkins, Recruited macrophages that colonize the post-inflammatory peritoneal niche convert into functionally divergent resident cells, Nat. Commun. 12 (1) (2021) 1770.

[26] O. Ernst, H. Failayev, M. Athamna, H. He, Y. Tsfadia, T. Zor, A dual and conflicting role for imiquimod in inflammation: a TLR7 agonist and a cAMP phosphodiesterase inhibitor, Biochem. Pharmacol. 182 (2020) 114206.

[27] M. Jin, T. Iwamoto, K. Yamada, H. Satsu, M. Totsuka, M. Shimizu, Disaccharide derived from chondroitin sulfate A suppressed CpG-induced IL-6 secretion in macrophage-like J774.1 cells, Cytokine 51 (1) (2010) 53–59.

[28] K. Onishi, J. Mochizuki, A. Sato, A. Goto, T. Sashihara, Total RNA and genomic DNA of Lactobacillus gasseri OLL2809 induce interleukin-12 production in the mouse macrophage cell line J774.1 via toll-like receptors 7 and 9, BMC Microbiol. 20 (1) (2020) 217.

[29] T.A. da Silva, A.L.V. Zorzetto-Fernandes, N.T. Cecílio, A. Sardinha-Silva, F. F. Fernandes, M.C. Roque-Barreira, CD14 is critical for TLR2-mediated M1 macrophage activation triggered by N-glycan recognition, Sci. Rep. 7 (1) (2017) 7083.

[30] A. Sodhi, S. Tarang, V. Kesherwani, Concanavalin A induced expression of Toll-like receptors in murine peritoneal macrophages in vitro, Int. Immunopharmacol. 7 (4) (2007) 454–463.

[31] F. Hayashi, K.D. Smith, A. Ozinsky, T.R. Hawn, E.C. Yi, D.R. Goodlett, J.K. Eng, S. Akira, D.M. Underhill, A. Aderem, The innate immune response to bacterial flagellin is mediated by Toll-like receptor 5, Nature 410 (6832) (2001) 1099–1103.

[32] A. Saviano, B. Apta, S. Tull, L. Pezhman, A. Fatima, M. Sevim, A. Mete, M. Chimen, A. Schettino, N. Marigliano, H.M. McGettrick, A.J. Iqbal, F. Maione, G.E. Rainger, PEPITEM, its tripeptide pharmacophores and their peptidomimetic analogues regulate the inflammatory response through parenteral and topical dosing in models of peritonitis and psoriasis, Pharm. Res. 213 (2025) 107624.

[33] A. Saviano, S. De Vita, M.G. Chini, N. Marigliano, G. Lauro, G.M. Casillo, F. Raucci, M. Iorizzi, R.K. Hofstetter, K. Fischer, A. Koeberle, O. Werz, F. Maione, G. Bifulco, In Silico, In Vitro, and In Vivo Analysis of Tanshinone IIA and Cryptotanshinone from Salvia miltiorrhiza as Modulators of Cyclooxygenase-2/mPGES-1/Endothelial Prostaglandin EP3 Pathway, Biomolecules 12 (1) (2022).

[34] F. Caso, A. Saviano, M. Tasso, F. Raucci, N. Marigliano, S. Passavanti, P. Frallonardo, R. Ramonda, V. Brancaleone, M. Bucci, R. Scarpa, L. Costa, F. Maione, Analysis of rheumatoid- vs psoriatic arthritis synovial fluid reveals differential macrophage (CCR2) and T helper subsets (STAT3/4 and FOXP3) activation, Autoimmun. Rev. 21 (12) (2022) 103207.

[35] V. Vellecco, A. Saviano, F. Raucci, G. Casillo, A. Abo Mansour, E. Panza, E. Mitidieri, G. Femminella, N. Ferrara, G. Cirino, R. Sorrentino, A. Iqbal, R. d'Emmanuele, di Villa Bianca, M. Bucci, F. Maione, Interleukin-17 (IL-17) triggers systemic inflammation, peripheral vascular dysfunction, and related prothrombotic state in a mouse model of Alzheimer's disease, Pharmacol. Res. 187 (2022) 106595.

[36] I.B.G.t. PHARMACOLOGY, 2025. ⟨https://www.guidetopharmacology.org/⟩. (Accessed 10th September 2025).

[37] I.G.t. immunopharmacology, 2025. ⟨https://www.guidetopharmacology.org/index.jsp⟩. (Accessed 10th September 2025).

[38] K. Zhang, J. Guo, W. Yan, L. Xu, Macrophage polarization in inflammatory bowel disease, Cell Commun. Signal 21 (1) (2023) 367.

[39] D.M. Mosser, J.P. Edwards, Exploring the full spectrum of macrophage activation, Nat. Rev. Immunol. 8 (12) (2008) 958–969.

[40] E.C. Butcher, Leukocyte-endothelial cell recognition: Three (or more) steps to specificity and diversity, Cell 67 (6) (1991) 1033–1036.

[41] L.R. Languino, A. Duperray, K.J. Joganic, M. Fornaro, G.B. Thornton, D.C. Altieri, Regulation of leukocyte-endothelium interaction and leukocyte transendothelial migration by intercellular adhesion molecule 1-fibrinogen recognition, Proc. Natl. Acad. Sci. 92 (5) (1995) 1505–1509.

[42] M. Beyer, M.R. Mallmann, J. Xue, A. Staratschek-Jox, D. Vorholt, W. Krebs, D. Sommer, J. Sander, C. Mertens, A. Nino-Castro, S.V. Schmidt, J.L. Schultze, High-resolution transcriptome of human macrophages, PLoS One 7 (9) (2012) e45466.

[43] J.S.Y. Tam, J.K. Coller, P.A. Hughes, C.A. Prestidge, J.M. Bowen, Toll-like receptor 4 (TLR4) antagonists as potential therapeutics for intestinal inflammation, Indian J. Gastroenterol. 40 (1) (2021) 5–21.

[44] F.J. Pérez-Cano, M. Massot-Cladera, M.J. Rodríguez-Lagunas, M. Castell, Flavonoids Affect Host-Microbiota Crosstalk through TLR Modulation, Antioxid. 3 (4) (2014) 649–670.

[45] S. Thomas-Ecker, A. Lindecke, W. Hatzmann, C. Kaltschmidt, K.S. Zänker, T. Dittmar, Alteration in the gene expression pattern of primary monocytes after adhesion to endothelial cells, Proc. Natl. Acad. Sci. 104 (13) (2007) 5539–5544.

[46] R.K. Gregg, J.J. Bell, H.H. Lee, R. Jain, S.J. Schoenleber, R. Divekar, H. Zaghouani, IL-10 diminishes CTLA-4 expression on islet-resident T cells and sustains their activation rather than tolerance, J. Immunol. 174 (2) (2005) 662–670.

[47] S. Huveneers, J. de Rooij, Mechanosensitive systems at the cadherin-F-actin interface, J. Cell Sci. 126 (Pt 2) (2013) 403–413.

[48] D. Vestweber, How leukocytes cross the vascular endothelium, Nat. Rev. Immunol. 15 (11) (2015) 692–704.

[49] M. Phillipson, P. Kubes, The neutrophil in vascular inflammation, Nat. Med. 17 (11) (2011) 1381–1390.

[50] A. Mantovani, A. Sica, S. Sozzani, P. Allavena, A. Vecchi, M. Locati, The chemokine system in diverse forms of macrophage activation and polarization, Trends Immunol. 25 (12) (2004) 677–686.
[51] J. Ortiz, K. Ragunath, Long-term survival after endoscopic resection for early gastric cancer in the remnant stomach: comparison with radical surgery, Ann. Gastroenterol. 28 (1) (2015) 1–2.
[52] M.F. Neurath, Cytokines in inflammatory bowel disease, Nat. Rev. Immunol. 14 (5) (2014) 329–342.
[53] M. Saraiva, A. O'Garra, the regulation of IL-10 production by immune cells, Nat. Rev. Immunol. 10 (3) (2010) 170–181.
[54] M. Nakaya, Y. Xiao, X. Zhou, J.H. Chang, M. Chang, X. Cheng, M. Blonska, X. Lin, S.C. Sun, Inflammatory T cell responses rely on amino acid transporter ASCT2 facilitation of glutamine uptake and mTORC1 kinase activation, Immunity 40 (5) (2014) 692–705.
[55] Y.R. Mahida, The key role of macrophages in the immunopathogenesis of inflammatory bowel disease, Inflamm. Bowel Dis. 6 (1) (2000) 21–33.
[56] Y.R. Na, M. Stakenborg, S.H. Seok, G. Matteoli, Macrophages in intestinal inflammation and resolution: a potential therapeutic target in IBD, Nat. Rev. Gastroenterol. Hepatol. 16 (9) (2019) 531–543.
[57] P.J. Koelink, F.M. Bloemendaal, B. Li, L. Westera, E.W.M. Vogels, M. van Roest, A. K. Gloudemans, A.B. van, T. Wout, H. Korf, S. Vermeire, A.A. Te Velde, C. Y. Ponsioen, G.R. D'Haens, J.S. Verbeek, T.L. Geiger, M.E. Wildenberg, G.R. van den Brink, Anti-TNF therapy in IBD exerts its therapeutic effect through macrophage IL-10 signalling, Gut 69 (6) (2020) 1053–1063.
[58] W.K.E. Ip, N. Hoshi, D.S. Shouval, S. Snapper, R. Medzhitov, Anti-inflammatory effect of IL-10 mediated by metabolic reprogramming of macrophages, Science 356 (6337) (2017) 513–519.
[59] M.M. Hu, H.B. Shu, Mitochondrial DNA-triggered innate immune response: mechanisms and diseases, Cell Mol. Immunol. 20 (12) (2023) 1403–1412.
[60] Y. Lu, X. Li, S. Liu, Y. Zhang, D. Zhang, Toll-like Receptors and inflammatory bowel disease, Front Immunol. 9 (2018) 72.
[61] E.J. Hennessy, A.E. Parker, L.A.J.O. Neill, Targeting Toll-like receptors: emerging therapeutics? Nat. Rev. Drug Discov. 9 (4) (2010) 293–307.
[62] S.C. Sun, The non-canonical NF-κB pathway in immunity and inflammation, Nat. Rev. Immunol. 17 (9) (2017) 545–558.